



**HAL**  
open science

# A Hierarchical Bayesian Examination of the Chronological Relationship between the Noaillian and Rayssian Phases of the French Middle Gravettian

William E Banks, Anaïs Vignoles, Jessica Lacarrière, André Morala, Laurent Klaric

► **To cite this version:**

William E Banks, Anaïs Vignoles, Jessica Lacarrière, André Morala, Laurent Klaric. A Hierarchical Bayesian Examination of the Chronological Relationship between the Noaillian and Rayssian Phases of the French Middle Gravettian. *Quaternary*, 2024, 7 (2), pp.26. 10.3390/quat7020026 . hal-04611951

**HAL Id: hal-04611951**

**<https://cnrs.hal.science/hal-04611951>**

Submitted on 14 Jun 2024

**HAL** is a multi-disciplinary open access archive for the deposit and dissemination of scientific research documents, whether they are published or not. The documents may come from teaching and research institutions in France or abroad, or from public or private research centers.

L'archive ouverte pluridisciplinaire **HAL**, est destinée au dépôt et à la diffusion de documents scientifiques de niveau recherche, publiés ou non, émanant des établissements d'enseignement et de recherche français ou étrangers, des laboratoires publics ou privés.

## Article

# A Hierarchical Bayesian Examination of the Chronological Relationship between the Noaillian and Rayssian Phases of the French Middle Gravettian

William E. Banks <sup>1,2,\*</sup> , Anaïs Vignoles <sup>3</sup>, Jessica Lacarrière <sup>4</sup> , André Morala <sup>1</sup> and Laurent Klaric <sup>4,\*</sup>

<sup>1</sup> University of Bordeaux, Centre National de la Recherche Scientifique (CNRS), Ministère de la Culture, PACEA, UMR 5199, F-33600 Pessac, France

<sup>2</sup> Biodiversity Institute, University of Kansas, 1345 Jayhawk Blvd, Lawrence, KS 66045, USA

<sup>3</sup> Service de Préhistoire, Université de Liège, 7 Place du XX Août, 4000 Liège, Belgium

<sup>4</sup> Université Paris X-Nanterre, Centre National de la Recherche Scientifique (CNRS), TEMPS, UMR 8068, 21 Allée de l'Université, 92023 Nanterre Cedex, France

\* Correspondence: william.banks@cnrs.fr (W.E.B.); laurent.klaric@cnrs.fr (L.K.)

**Abstract:** Issues of chronology are central to inferences pertaining to relationships between both contemporaneous and successive prehistoric typo-technological entities (i.e., archaeological cultures), culture–environment relationships, and ultimately the mechanisms at play behind cultural changes observed through time in the archaeological record. We refine the chronology of Upper Paleolithic archaeological cultures between 35–18 calibrated kiloanni before the present in present-day France by incorporating recently published radiocarbon data along with new <sup>14</sup>C ages that we obtained from several Gravettian archaeological contexts. We present the results of a Bayesian age model that includes these new radiometric data and that, more importantly, separates Gravettian contexts in regions north of the Garonne River into two successive cultural phases: The Northern Noaillian and the Rayssian, respectively. This new age model places the beginning of the Noaillian during Greenland Stadial 5.2. The appearance of contexts containing assemblages associated with the Rayssian lithic technical system occurs immediately prior to the termination of Greenland Interstadial 5.1, and it is present throughout Heinrich Event 3 (GS-5.1) and into the following GI-4 climatic amelioration. Despite the Rayssian's initial appearance during the brief and relatively weakly expressed Greenland Interstadial 5.1, its duration suggests that Rayssian lithic technology was well-suited to the environmental conditions of Greenland Stadial 5.1.

**Keywords:** Middle Gravettian; Noaillian; Rayssian; chronology; hierarchical Bayesian age modeling; ChronoModel; Heinrich Stadial 3



**Citation:** Banks, W.E.; Vignoles, A.; Lacarrière, J.; Morala, A.; Klaric, L. A Hierarchical Bayesian Examination of the Chronological Relationship between the Noaillian and Rayssian Phases of the French Middle Gravettian. *Quaternary* **2024**, *7*, 26. <https://doi.org/10.3390/quat7020026>

Academic Editors: Frank Sirocko, Pierre Antoine and María Fernanda Sánchez Goñi

Received: 3 March 2024  
Revised: 31 May 2024  
Accepted: 31 May 2024  
Published: 12 June 2024



**Copyright:** © 2024 by the authors. Licensee MDPI, Basel, Switzerland. This article is an open access article distributed under the terms and conditions of the Creative Commons Attribution (CC BY) license (<https://creativecommons.org/licenses/by/4.0/>).

## 1. Introduction

Issues of chronology are paramount in efforts to make reliable inferences pertaining to relationships between both contemporaneous and successive prehistoric typo-technological entities (i.e., archaeological cultures), culture–environment relationships, and ultimately the mechanisms at play behind cultural changes observed in the archaeological record [1]. This is especially true in contexts characterized by millennial and sub-millennial climatic variability, such as the Middle and Upper Paleolithic contexts of Marine Isotope Stages 3 and 2, since past hunter-gatherer cultures operated within environmental contexts that potentially influenced, to varying degrees, the cultural variability we observe [2–6].

In a previous study, Banks and colleagues [1] examined all radiocarbon measurements from reliable archaeological contexts (i.e., radiocarbon ages with secure determinations of archaeological association) in the region of Europe that is bounded to the south by the Pyrenees, the Atlantic Ocean to the West, and the Alps and Jura Mountains to the east. The goal was to determine the chronology of the different typo-technological phases that make up the

Gravettian, Solutrean, and Badegoulian technocomplexes and to correlate these different archaeological cultures' chronological intervals with documented paleoclimatic variability. Their analysis could not provide a detailed examination of the typo-technological phases that make up the Middle Gravettian due to a paucity of reliable radiocarbon ages from such contexts, as well as uncertainties at that time with respect to the Middle Gravettian phase attributions of archaeological levels and numerous sites. Analyses carried out by Vignoles [6] have lent precision to the typo-technological attributions for a number of these Gravettian archaeological contexts. These cultural attributions allow for the construction of chronologies, or at least the exploration of potential chronologies, that differentiate certain archaeological cultural phases that could not be reliably differentiated previously.

The objective of this article is three-fold. First, we present 23 new radiocarbon measurements from five Gravettian contexts: the rock shelters of Le Facteur, Le Flageolet I, and Le Callan, and the open-air sites of Les Jambes and La Picardie. Second, we evaluate the results presented by Banks et al. [1] against those obtained by injecting newly obtained radiocarbon measurements into the previously published age model structure. A number of these new data are the measurements presented here, and the remaining are those published by others since the publication of Banks et al.'s model. Since the Bayesian hierarchical method that we employ is based on the Event Date concept and allows for the construction of a single age model that takes into account all radiometric observations and their associated priors (described in detail below), we expect that the injection of a large number of new radiocarbon measurements into the previously published model will result in a cultural chronology that differs only slightly from the original. Last, we explore the chronological relationship between the Noaillian and Rayssian phases of the Middle Gravettian north of the Garonne River (France) via the creation of an age-model structure in which relevant radiocarbon measurements are placed into one of the two successive cultural phases.

This last aim was not possible previously since ages that could be unequivocally attributed to either the Noaillian or Rayssian were insufficient in number. Following recent evaluations of a number of Middle Gravettian archaeological assemblages [6] and by employing an age-model structure that reflects the hypothesis that the Rayssian succeeds the Noaillian in regions north of the Garonne River, we can propose chronological intervals for these two cultural phases. The obtained chronological interval for the Rayssian will also allow us to test the hypothesis that its characteristic technical system is correlated with Heinrich Event 3 [ca. 30–29 calibrated kiloanni Before Present (cal ka BP); [7–11]], as initially proposed by Banks et al. [1].

#### *French Middle Gravettian*

As one of the goals of this study is to evaluate the chronological relationship between the two cultural taxonomic units (i.e., archaeological cultures) observed in the Middle Gravettian archaeological record of present-day France, it is necessary to describe briefly these two entities—the Noaillian and the Rayssian—and their associated archaeological records (Figure 1). During the chronological interval situated between ca. 31–28.5 cal ka BP, in present-day France, are the Noaillian and Rayssian archaeological phases, often referred to as “*faciès*” by the French archaeological community, and they are defined principally on the characteristics of their associated lithic industries [12]. The definition of the “Middle Gravettian”, as well as its internal subdivisions (Noaillian and Rayssian) in northern Aquitaine, is historically linked to the excavations of the Abri Pataud in Dordogne [13]. Under the term “Noaillian”, N. David and H.M. Movius chronologically subdivided the various lenses of Level 4 into “Lower Noaillian” (Noaillian *stricto sensu* or Noailles burin *faciès*) and “Upper Noaillian” (Rayssian burin-core *faciès*) [14]. The term “Rayssian” was proposed by other authors to designate the “Upper Noaillian” [15] and has been used more widely since [16,17]. The inventory of Gravettian sites with Noailles burins (Noaillian *stricto sensu*) includes 109 sites spread from Cantabria to western Italy, including a good portion of southern France [12]. Only 26 sites attributed to the Rayssian are known and

are located exclusively in France [18]. When encountered in sequence, the Rayssian lies between the Noaillian *stricto sensu* and the Late Gravettian (e.g., Abri Pataud, Le Flageolet). In two stratigraphic sequences (Taillis des Côteaux and Les Jambes), the Rayssian appears to precede the Noaillian; however, post-depositional processes paired with the fact that the results of these excavations have only been partially published likely explain this unusual inversion [6,19].

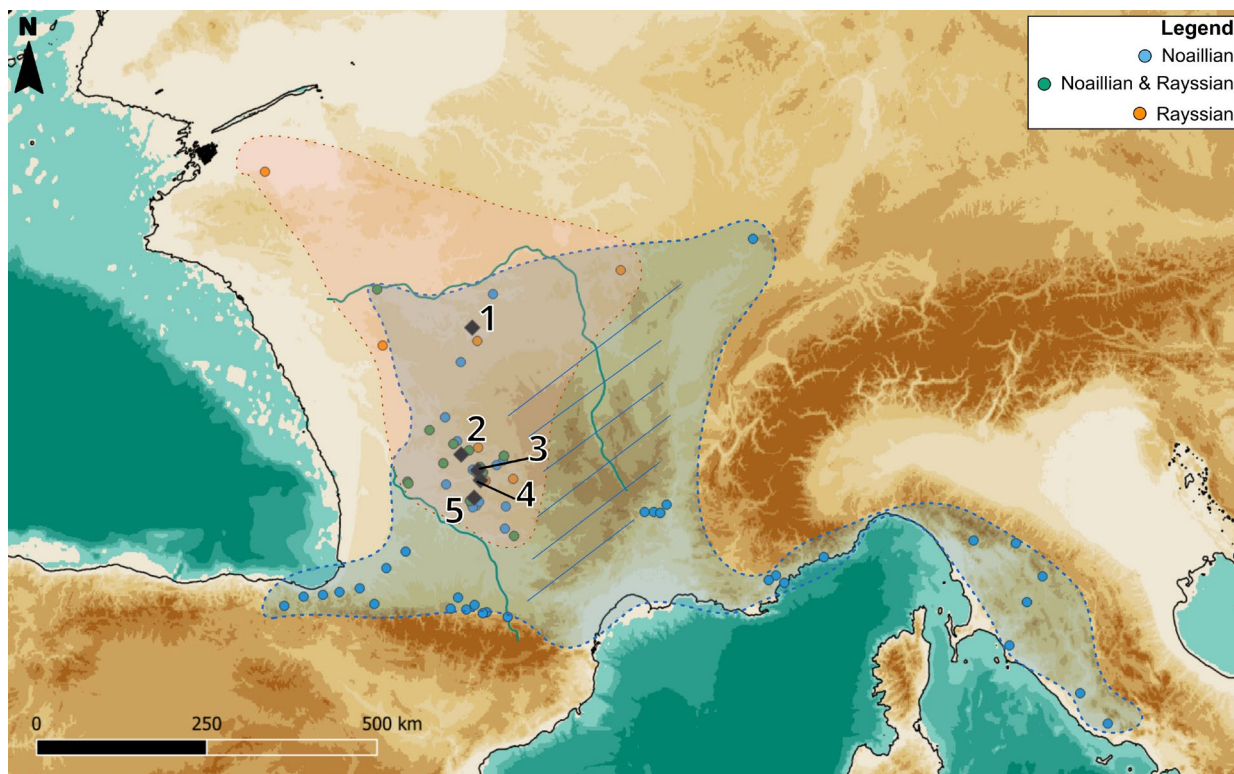


**Figure 1.** Geographic extents of the Noaillian and Rayssian techno-complexes, in blue and orange, respectively. Locations of archaeological contexts attributed to the Noaillian are indicated with blue circles. Sites with Rayssian archaeological levels are indicated by orange circles. Sites where both techno-complexes have been observed are indicated with green circles. The sites from which samples were selected for  $^{14}\text{C}$  dating in the context of this study are numbered: (1) La Picardie; (2) Les Jambes; (3) Le Facteur; (4) Le Flageolet I; (5) Callan. Sea levels are depicted at  $-90$  m below sea level, corresponding to approximately 30 ka cal BP [20].

Lithic diagnostics typologically characteristic of the Noaillian (Noailles burins, Gravette points, microgravettes, and truncated-backed bladelets) and the Rayssian (Raysse burin-core, la Picardie bladelets, and Raysse bladelets) are often found together within the same archaeological levels [6,16,17,21,22] (Figure 2). These associations have supported the hypothesis of close functional and chronological links between the two [16,17]. However, complex taphonomic processes linked to the dynamics of rock shelter formation and accumulation, as well as periglacial conditions or even less rigorous excavation methods, can explain such associations [6,23–25]. There remains, however, a lack of consensus [26,27], and the nature of the observed associations between Noailles burins, Raysse burin-cores, Picardie bladelets, and Gravette points remains unresolved. Furthermore, the Noaillian and Rayssian refer to two different archaeological realities [28]. The Noaillian is most typically defined by the presence of a single lithic artifact type, the Noailles burin, which leads to it being less well-characterized due to the fact that Noaillian burins have broad chronological and geographic extents (Figure 1). On the contrary, the Rayssian is a more coherent entity due to the fact that it is defined on the basis of not only diagnostic lithic elements—Raysse burin-cores and Picardie bladelets—but also the lithic technical system particular to these

two diagnostic elements, thereby making it a more coherent technical unity [16,17,22,29]. In addition to this is the fact that the Rayssian appears better constrained geographically (Figure 1).

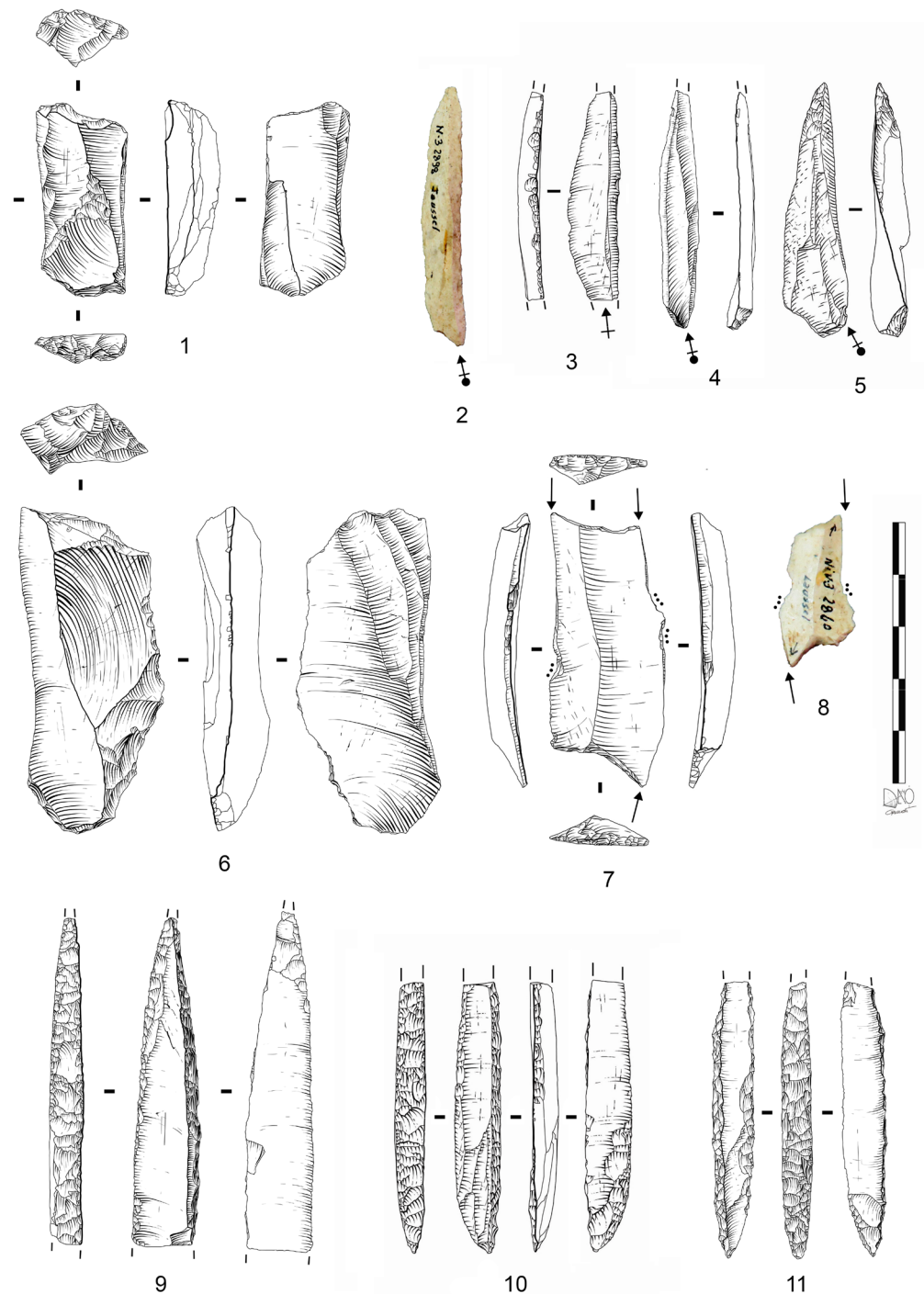


**Figure 2.** Principal French Middle Gravettian typo-diagnostic lithic artifacts (Laussel, Dordogne: Lalanne, Vésignié, and Daniel collections); n° 1 and 6: Raysse burin-cores; n° 2 and 3: La Picardie bladelets; n° 4 and 5: Raysse bladelets; n° 7 and 8: Noailles burins; n° 9: Gravette point (Vachons sub-type); n° 10 and 11: microgravette points (Vachons sub-type). Barred arrows represent the direction of removal and a solid circle at the arrow's origin indicates that the platform is present. Plain arrows indicate a burin spall's direction of removal. A series of three dots (n° 7 and 8) indicates retouch meant to stop a burin spall's propagation. Drawings by P. Gaussein. Photography by L. Klaric.

Over the past fifty years, three interpretative hypotheses have been proposed to explain the relationship between Middle Gravettian lithic industries in present-day France and immediately adjacent regions. First, some propose a continuity between the Noaillian and Rayssian [13,30–32]. A second hypothesis proposes a degree of functional complementarity between the two [27,33–35]. The third is founded on the idea of a cultural break between the Noaillian *stricto sensu* and the Rayssian [16,29]. None of these, however, are particularly convincing since they all rely exclusively on the lithic archaeological record [17]. More recently, new avenues have been raised, suggesting possible environmental reorganizations (faunal, permafrost extension, etc.) in northern areas during Heinrich Event (HE) 3, which occurred during Greenland Stadial (GS) 5.1 [1]. Perhaps such changes exerted a non-negligible (but not exclusive) influence on the behaviors and adaptations of Middle Gravettian human groups [6,36]. A cautious position at present is to consider that the Rayssian (in Northern Aquitaine) is contemporaneous with the Pyrenean Noaillian and that they are contemporaneous cultural expressions during the second half of the Middle Gravettian. If there is any chronological phasing, it is only in the Northern Aquitaine area that it is currently perceptible, even if it remains difficult to determine precisely in terms of absolute chronology. Here, our operating hypothesis—founded on analyses of archaeological contexts—is that the emergence of the Rayssian represents a technical rupture with the Noaillian and that the Rayssian contexts postdate those of the Noaillian in the area of present-day northern Aquitaine and in regions to the north, as is observed in the sequence of lenses that make up layer 4 at Pataud shelter, for example. Based on this hypothesis, we create an appropriately structured Bayesian age model in order to propose a tentative chronology for the Rayssian technical system, which will allow for a better understanding of its correlation with the chronology of millennial-scale climatic variability and corresponding environments.

## 2. Materials and Methods

### 2.1. Chronological Data

A large portion of the chronological data employed in this study is composed of the  $^{14}\text{C}$  ages used in the hierarchical Bayesian age modeling analysis previously conducted by Banks et al. [1]. Since the publication of that model and its results, numerous radiocarbon measurements that fall within its chronological interval have been published [37,38]. To complement these existing data and pursue the objectives of this analysis, we sampled a number of Gravettian archaeological levels from five sites (Figure 1), two of which have never been the subject of radiometric dating efforts (Les Jambes and La Picardie), in order to obtain bone and charcoal samples for radiocarbon measurements, with the majority of the former bearing anthropogenic traces (Table 1). Below, we briefly present the archaeological contexts associated with our samples.

#### 2.1.1. Le Callan

The site of Le Callan is situated in the commune of Blanquefort-sur-Briolance in the Lot-et-Garonne Department of southwestern France. It is composed of four Gravettian levels, with the upper two containing lithic assemblages that can be attributed to the Noaillian phase of the Middle Gravettian. Recovered from the lower two levels are Gravettian lithic assemblages dominated by microgravettes [39,40]. While a cultural attribution for the lower two levels has not been formally proposed, due to their stratigraphic position below the Noaillian levels, it is likely that they represent either Early Gravettian occupations or transitional ones immediately preceding the appearance of the Noaillian *faciès*. Because the upper levels, I and II, share the same Noaillian lithic industry and the lower levels, III and IV, share the same unattributed industry, they have been grouped together into two broad archaeological units, I–II and III–IV.

**Table 1.** Archaeological samples from Gravettian contexts submitted to the Oxford radiocarbon accelerator unit for dating. Table also available at <https://doi.org/10.48579/PRO/U1GKGW>.

| Site           | Arch. Level | Unit/Square | Sample ID   | Artifact Code | Material | Taxon                         | Anatomical Element | Portion                  | Human Modification                  | Mass (g) | %N   | Notes                            |
|----------------|-------------|-------------|-------------|---------------|----------|-------------------------------|--------------------|--------------------------|-------------------------------------|----------|------|----------------------------------|
| Le Callan      | IV          | F4          | Callan-1    | 76            | bone     | Cervidae                      | Possible femur     | diaphysis fragment       | None                                | 3.5      | 0.22 | Sample withdrawn                 |
| Le Callan      | IV          | F4          | Callan-2    | 211           | bone     | <i>Rangifer tarandus</i>      | femur              | diaphysis fragment       | Burned; green bone break            | 1.2      | 0.34 | Sample withdrawn                 |
| Le Callan      | I-II        | H4          | Callan-3    | 77            | bone     | <i>Rangifer tarandus</i>      | Radius or femur    | diaphysis fragment       | Abraded; cutmarks                   | 5.7      | 0.46 | Radiocarbon measurement obtained |
| Le Callan      | I-II        | G4          | Callan-4    | 224           | bone     | <i>Rangifer tarandus</i>      | Humerus            | diaphysis fragment       | green bone break                    | 6.5      | 0.60 | Radiocarbon measurement obtained |
| Le Callan      | I-II        | G4          | Callan-5    | 181           | bone     | Cervidae ( <i>Rangifer?</i> ) | Cranium            | possible petrus fragment | Burned; green bone break            | 3.2      | 0.30 | Sample withdrawn                 |
| Le Callan      | I-II        | H6A         | Callan-6    | 11            | bone     | <i>Rangifer tarandus</i>      | Right P3/P4        | complete                 | None                                | 2.9      | 0.37 | Sample withdrawn                 |
| Le Facteur     | J-11        | Sond. 72    | Facteur-1   | 78            | bone     | <i>Cervus elaphus</i>         | Left femur         | diaphysis                | Cutmarks; green bone break          | 12.0     | 0.26 | Sample withdrawn                 |
| Le Facteur     | J-11        | Sond. 72    | Facteur-2   | 23            | bone     | <i>Rangifer tarandus</i>      | Metatarsal         | proximal, medial         | Abraded; green bone break           | 10.0     | 0.40 | Radiocarbon measurement obtained |
| Le Facteur     | J-11        | Sond. 72    | Facteur-3   | 121           | bone     | <i>Rangifer tarandus</i>      | Metatarsal         | medial diaphysis         | Green bone break; possible cutmarks | 9.0      | 0.61 | Radiocarbon measurement obtained |
| Le Facteur     | J-11        | Sond. 72    | Facteur-4   | 300           | bone     | <i>Rangifer tarandus</i>      | Long bone          | medial diaphysis         | Green bone break                    | 3.0      | 0.29 | Sample withdrawn                 |
| Le Flageolet I | VII         | C9          | Flageolet-1 | 1881          | bone     | <i>Cervus elaphus</i>         | Left humerus       | medial diaphysis         | Abraded                             | 11.0     | 0.45 | Radiocarbon measurement obtained |
| Le Flageolet I | VII         | C10         | Flageolet-2 | 1220          | bone     | <i>Cervus elaphus</i>         | Right femur        | diaphysis fragment       | Cutmarks                            | 13.8     | 0.29 | Sample withdrawn                 |

Table 1. Cont.

| Site           | Arch. Level | Unit/Square | Sample ID    | Artifact Code | Material | Taxon                    | Anatomical Element | Portion             | Human Modification        | Mass (g) | %N   | Notes  |
|----------------|-------------|-------------|--------------|---------------|----------|--------------------------|--------------------|---------------------|---------------------------|----------|------|--|
| Le Flageolet I | VII         | C10         | Flageolet-3  | 1185          | bone     | Bovid                    | 1st phalange       | distal              | Cutmarks                  | 15.9     | 0.43 | Radiocarbon measurement obtained                                 |
| Le Flageolet I | VI          | C8          | Flageolet-5  | 877           | bone     | Size IV herbivore        | Long bone          | diaphysis fragment  | Cutmarks                  | 18.5     | 0.90 | Radiocarbon measurement obtained; VSG—very small graphite target |
| Le Flageolet I | VI          | C7          | Flageolet-6  | 763           | bone     | Bovid                    | Metatarsal         | diaphysis fragment  | Cutmarks                  | 41.6     | 0.39 | Radiocarbon measurement obtained                                 |
| Le Flageolet I | VI          | C7          | Flageolet-7  | 607           | bone     | <i>Rangifer tarandus</i> | 1st phalange       | complete            | Cutmarks                  | 9.6      | 0.84 | Radiocarbon measurement obtained                                 |
| Le Flageolet I | VI          | C7          | Flageolet-8  | 809           | bone     | <i>Rangifer tarandus</i> | Metatarsal         | diaphysis fragment  | Cutmarks                  | 5.0      | 1.60 | Radiocarbon measurement obtained                                 |
| Le Flageolet I | V           | C10         | Flageolet-10 | 480           | bone     | <i>Equus ferus</i>       | Left tibia         | anterior diaphysis  | Abraded; likely retoucher | 38.3     | 0.88 | Radiocarbon measurement obtained                                 |
| Le Flageolet I | V           | C10         | Flageolet-11 | 449           | bone     | <i>Rangifer tarandus</i> | Left tibia         | diaphysis fragment  | None                      | 11.7     | 0.90 | Radiocarbon measurement obtained                                 |
| Le Flageolet I | V           | C9          | Flageolet-12 | 744           | bone     | <i>Rangifer tarandus</i> | Right radius       | diaphysis fragment  | Cutmarks                  | 11.5     | 0.75 | Radiocarbon measurement obtained                                 |
| Le Flageolet I | V           | C9          | Flageolet-13 | 726           | bone     | <i>Rangifer tarandus</i> | Radius             | anterior diaphysis  | Abraded                   | 9.8      | 0.80 | Radiocarbon measurement obtained; Very small reindeer            |
| Le Flageolet I | V           | C10         | Flageolet-14 | 315           | bone     | <i>Rangifer tarandus</i> | Right humerus      | posterior diaphysis | Cutmarks; abraded         | 7.9      | 0.48 | Radiocarbon measurement obtained                                 |



Table 1. Cont.

| Site           | Arch. Level | Unit/Square | Sample ID    | Artifact Code | Material | Taxon                    | Anatomical Element | Portion             | Human Modification | Mass (g) | %N   | Notes  |
|----------------|-------------|-------------|--------------|---------------|----------|--------------------------|--------------------|---------------------|--------------------|----------|------|--|
| Le Flageolet I | IV          | C9          | Flageolet-19 | 415           | bone     | <i>Rangifer tarandus</i> | Tibia              | posterior diaphysis | None               | 3.3      | 0.36 | Sample withdrawn   |
| Le Flageolet I | IV          | C6          | Flageolet-20 | no number     | bone     | <i>Rangifer tarandus</i> | Right tibia        | lateral diaphysis   | Possible cutmarks  | 7.2      | 0.52 | Measurement failed   |
| Le Flageolet I | IV          | C6          | Flageolet-21 | no number     | bone     | <i>Rangifer tarandus</i> | Left tibia         | diaphysis fragment  | Cutmarks           | 9.0      | 0.51 | Radiocarbon measurement obtained; VSG—very small graphite target |
| Le Flageolet I | VI          | B10         | Flageolet-22 | 987           | bone     | <i>Cervus elaphus</i>    | Left humerus       | diaphysis fragment  | None               |          | 0.46 | Measurement failed   |
| Les Jambes     | 3           | B0          | Jambes-1     | no number     | bone     | <i>Equus?</i>            | Humerus            | fragment            | None               | 54.7     | 0.58 | Radiocarbon measurement obtained                                 |
| Les Jambes     | 3           | B           | Jambes-2     | no number     | bone     | <i>Rangifer tarandus</i> | Tooth              | complete            | None               | 3.5      | 0.42 | Radiocarbon measurement obtained                                 |
| Les Jambes     | 2           | indet.      | Jambes-3     | no number     | bone     | <i>Rangifer tarandus</i> | Scapula            | fragment            | None               | 16.9     | 0.36 | Sample withdrawn   |
| Les Jambes     | 2           | indet.      | Jambes-4     | no number     | bone     | <i>Equus?</i>            | Possible tibia     | fragment            | None               | 27.8     | 1.30 | Radiocarbon measurement obtained                                 |
| Les Jambes     | 3           | B           | Jambes-5     | B155          | bone     | <i>Rangifer tarandus</i> | Left humerus       | distal              | None               | 21.0     | 1.09 | Radiocarbon measurement obtained                                 |
| Les Jambes     | 3           | B           | Jambes-6     | B157          | bone     | <i>Equus</i>             | Radius             | proximal            | None               | 89.0     | 0.26 | Sample withdrawn   |
| La Picardie    | c2d3        | F97D        | Picardie-3   |               | charcoal | <i>Pinus</i>             | n/a                | n/a                 | n/a                |          |      | Measurement failed   |
| La Picardie    | c2na1       | G10A        | Picardie-4   |               | charcoal | <i>Quercus</i>           | n/a                | n/a                 | n/a                | 5.5      |      | Radiocarbon measurement obtained                                 |

In an effort to establish the chronological age of the site's two broad archaeological units, we chose five bone fragments and a reindeer tooth for radiocarbon dating (Table 1). Two of these pieces are from level IV and the remaining four are from the combined unit I–II. Faunal remains from the site are few in number, and those that appeared to be most promising for obtaining a  $^{14}\text{C}$  age were selected, although the scarcity of datable material required that we include two burned bone fragments. We attribute the  $^{14}\text{C}$  ages from this site to the Noaillian taxonomic unit of the Middle Gravettian.

### 2.1.2. Le Facteur

The Le Facteur rockshelter is situated within the commune of Tursac in the Dordogne Department of southwestern France. After having been investigated by various amateur archaeologists, Elie Peyrony first conducted formal scientific excavations at the site in 1933 [41], and further fieldwork was conducted by Henri Delporte during the latter half of the 1950s. These latter excavations were conducted with relatively modern techniques and in his synthesis, Delporte [42] defined 22 archaeological levels. He assigned levels 10 and 11 to the “Périgorien supérieur à burins de Noailles”, now termed the Noaillian phase of the Middle Gravettian. These two levels were defined on the basis of different sedimentary characteristics, but they were in direct contact with one another and situated near the back of the rockshelter, thus making it difficult to unequivocally demonstrate their individual integrity. For this reason, they are often referred to as level 10/11. While Noaillian burins are abundant in this archaeological unit, Deporte's analytical method was not conducive to recognizing lithic elements now known to belong to the Rayssian phase of the Middle Gravettian. Analyses of this assemblage conducted during the 1980s [14] recognized artifacts that are diagnostic of the Rayssian, and more recent, detailed examinations of the assemblage [6,25] confirm that, in addition to Noaillian diagnostics, Deporte's level 10/11 contains a small number of Raysse burin-cores along with a few Raysse and Picardie bladelets, which are characteristic of lithic reduction sequences performed on Raysse burin-cores. However, the blade reduction sequence is very similar to that of Noaillian assemblages present in the Landes-Pyrenees area (e.g., Brassempouy) [16,43], and another reduction sequence for the production of marginally retouched bladelets from burin-cores—different from the Raysse method—is also present. In this context, the presence of elements produced with the Raysse method is difficult to interpret.

While it is not possible to differentiate between the Noaillian and Rayssian occupations represented in the combined “level” 10/11 at Le Facteur, we still deemed it worthwhile to obtain radiocarbon measurements since they could provide useful chronological data for the Middle Gravettian as a whole. To this end, we selected four faunal remains for dating from Chantier J sondage (square meter test pit) 72 (Table 1), which was excavated in 1958 and for which excavation notes are available (curated in the archives of the Musée d'Archéologie Nationale in Saint-Germain-en-Laye, France). All four samples are indicated to be from the stratigraphically lower, and thus older, level 11, although as pointed out above, reliably associating dated materials to one of the two levels is difficult. For this study, this combined “level” 10/11 is attributed to the Noaillian phase.

### 2.1.3. Le Flageolet I

The site of Le Flageolet I is the westernmost of two neighboring rock shelters situated in the commune of Bézenac in the Dordogne Department of southwestern France. The site was excavated by Jean-Philippe Rigaud between 1968 and 1984 using modern excavation methods [27,33,44]: artifacts larger than 1.5 cm were piece-plotted and excavated sediments were sieved in order to recover smaller elements. Stratigraphic attributions were controlled via on-site sagittal and longitudinal projections. It contains a stratified archaeological sequence for the early Upper Paleolithic composed of three archaeological levels attributed to the Aurignacian (XI, IX, and VIII) in lithostratigraphic unit I, and above these are six levels attributed to the Gravettian (VII, VI, V, IV, I–III, and 0) contained in lithostratigraphic unit II [27].

A recent examination of levels I–III, IV, V, and VI permitted an update to their cultural attributions [6]. Rayssian diagnostic artifacts are numerous in levels I–III, IV, and V, while Noaillian *fossiles directeurs* are rare. In level V, blade and bladelet reduction sequences are characterized by mixed characteristics between the Rayssian and the Pyrénées Noaillian [45]. As is observed in the sagittal projections, the presence of rare Noaillian and Rayssian artifacts in levels VI and VII is more likely due to post-depositional processes or to stratigraphic re-attributions of the remains. Furthermore, backed bladelet characteristics differ between levels I–III/IV/V and VI/VII. The latter levels also yield more typologically diversified assemblages that include lithic artifact types diagnostic of the Early Gravettian (truncated elements, Tursac points, and alternate backed points). Sagittal projections of piece-plotted artifacts and refitting analyses indicate the presence of two main concentrations that correspond to levels I–III/IV/V and levels VI/VII. These two stratigraphic groupings are separated by a layer in which artifacts are sparse. The former ensemble corresponds to the Middle Gravettian, while the second can be attributed to the Early Gravettian. In this context, the association of backed points together with Rayssian artifacts and a handful of Noaillian elements in the upper levels is difficult to interpret but is likely due to the palimpsest nature of the deposits and post-depositional processes [6].

When selecting samples for radiocarbon measurements, we targeted the C transect of the site's grid and focused on grid units situated in the southern portion of the excavated area (e.g., C6–C10; see [27]). Since the archaeological levels are fairly thin and in close proximity to, or in contact with, one another, we consulted the depth coordinates of individual piece-plotted faunal remains and selected those that were situated towards the middle portion of their associated archaeological level. This was done in order to minimize the selection of samples from areas representing the contact zone between two archaeological levels. We sampled three faunal elements from level VII, five from level VI, five from level V, and three from level IV (Table 1).

As cited above, the diagnostics described from levels VII and VI lead us to attribute them to the Early Gravettian, and based on the fact that elements diagnostic of the Rayssian are predominant in le Flageolet I levels V and IV, we attribute these two levels to the Rayssian phase of the Middle Gravettian.

#### 2.1.4. Les Jambes

The site of Les Jambes is located in slope deposits in the northwestern sector of the city of Périgueux on the right bank of the Isle River in southwestern France. It was excavated by Guy Célérier from 1964–1968, and the excavated surface totaled 13 m<sup>2</sup>, although the only published description of the work concerns the first two field campaigns for which only four square meters were excavated [46]. Célérier describes three stratigraphic units, numbered 1–3 from top to bottom, with the lower two each containing a single archaeological level, both of which he attributed to the Noaillian based on the presence of eight Noailles burins and the frequencies of other tool types typical of other Middle Gravettian assemblages. A previous examination of the recovered lithic assemblages [14] and a more recent assessment based on Célérier's published drawings [16], however, suggested that the Rayssian *faciès* is strongly expressed. Vignoles [6] confirmed the Rayssian cultural attribution based on the presence of diagnostic elements and lithic reduction strategies. Vignoles [6] also demonstrates that of the 15 "Noailles burins" identified by Célérier, only one can be classified as such, thereby indicating that the site's levels are predominantly Rayssian.

With respect to Célérier's interpretation that the site's stratigraphy was inverted—a hypothesis based on his identification of Noailles burins in level 2 and their absence in the lower level 3—it has been proposed that this apparent inversion is the result of the post-depositional processes of the site's sloped deposits [14,16]. Following a revision of the site's assemblages and excavation notes, Vignoles [6] concludes that the available data invalidate the inversion hypothesis. First, Célérier notes the presence of Noailles burins in level 3 in his 1967 field report, which was not included in his subsequent publication [46]. Second, the so-called (and revised) Noailles burins are only present in level 3. The presence

of the one true Noailles burin, the two atypical burins, as well as a busked burin typical of the Recent Aurignacian, indicates that some intrusive elements from earlier, ephemeral occupations at the site are present in these two purported Rayssian Middle Gravettian levels. An examination of artifact distributions clearly indicates the sloped nature of the deposits and suggests that the site may in fact only contain a single archaeological level instead of the purported two [6].

We selected six faunal remains, representing a range of taxa (Table 1). Two of the specimens are from Célérier's level 2, and the remaining four were recovered from level 3. Unfortunately, while provenience data from the excavation records did allow us to determine their archaeological level of origin, it was not possible to determine from where in their respective levels they were originally recovered.

Despite a recommendation that dates not be attributed to a specific Middle Gravettian *faciès* [6], we attribute the  $^{14}\text{C}$  ages from Les Jambes to the Rayssian phase. The reason behind this decision is the fact that examinations of its two recognized archaeological levels—which may, in fact, represent a single level—demonstrate that the lithic assemblage is dominated by a lithic industry that is similar to that observed in the upper Middle Gravettian assemblages at Le Flageolet I (levels V, IV, and III-I), which are predominantly Rayssian in character with rare Noailles burins and backed points.

#### 2.1.5. La Picardie

La Picardie is an open-air site located in the commune of Preuilly-sur-Claise in the Indre-et-Loire Department. It was discovered in the late 1990s and subjected to several field-work campaigns from 2003–2008, over which time 84 square meters were excavated [47,48]. La Picardie is a single-component site whose lithic assemblage is attributed solely to the Rayssian phase of the Middle Gravettian due to the presence of this phase's lithic diagnostic artifacts, and it is also characterized by an absence of Gravette points, microgravettes, and Noailles burins [16]. This is the eponymous site for the Picardie bladelet, which is a marginally retouched bladelet—employed as a hunting armature—removed from a Raysse burin-core [49].

Due to its open-air context and clay-rich sediments, no faunal remains are preserved, making precise determinations of this site's age challenging. In the framework of this study, two small fragments of charcoal recovered from the archaeological level were submitted for dating (Table 1) in the hopes that they would provide radiocarbon ages for an archaeological context that is solely Rayssian.

#### 2.2. Radiocarbon Sample Treatment and Measurement Methodology

All bone and charcoal samples obtained from the archaeological contexts described above were sent to the Oxford Radiocarbon Accelerator Unit. The majority of our samples were faunal skeletal elements from which collagen was extracted following the pretreatment protocol described by Brock et al. [50]. The charcoal samples from La Picardie were pretreated with the relevant protocol. Following pretreatment, samples were graphitized [51] and then dated on the ORAU HVEE AMS system [52].

Of the 34 samples sent for dating, 32 were archaeological faunal remains and part of the pretreatment protocol to which they were subjected consisted of a %N screening. Only nine of the samples have %N values above 0.7. Samples with such a value have a roughly 85% chance of having sufficient collagen for an ultrafiltration radiocarbon determination. This represents less than a third of the submitted samples; therefore, we decided to pursue obtaining non-ultrafiltered dates by also retaining samples with %N values between 0.4–0.7. Based on the %N results, we also withdrew a number of samples: four from the site of Le Callan, two from Le Facteur, two from Le Flageolet I, and two from Les Jambes (Table 1).

#### 2.3. Hierarchical Bayesian Age Modeling with ChronoModel

During the past three decades, the archaeological community has increasingly relied on Bayesian methods for constructing cultural chronologies as these methods allow one to

take into account stratigraphic information (i.e., priors), which serves to render chronologies more robust and accurate [53–58]. Banks et al. [1] describe an approach that uses the software package ChronoModel (Version 2.0) [58,59] to construct a nested hierarchical Bayesian age model that allows all archaeologically reliable chronological data, from both stratified archaeological sequences and single component sites, to be incorporated into a single model structure in a statistically robust manner. Such a model structure overcomes the statistical problems associated with the approach that consists of constructing separate age models for individual sequences and injecting, into a new model, the a posteriori probability distributions corresponding to the boundaries between phases that represent a change in archaeological cultural traditions. Such a model is composed of chronologically ordered phases, each representing one of the archaeological cultural transitions in question [60,61]. The problem with this approach is that the second-generation model is populated with a posteriori probability distributions that are derived from the individual site age models, thereby introducing additional unknown boundaries as priors. Such an approach is statistically undesirable.

The age model and examination of cultural chronology described by Banks et al. [1] targeted the portion of the Upper Paleolithic between 32–21 cal ka BP. They highlight the fact that numerous, dated archaeological contexts (i.e., archaeological levels) are associated with formation or post-depositional processes that make it difficult to examine the chronological relationship between the two typo-technological units, the Noaillian and the Rayssian, attributed to the Middle Gravettian in areas north of the Garonne River. They postulate that, in these areas, the Rayssian post-dates the Noaillian and is chronologically situated during the latter portion of the Middle Gravettian, an interval corresponding to Heinrich Event 3, but that more data are needed in order to better establish the relationship between these two technical systems.

Bayes theorem allows one to combine chronological probabilistic information (e.g., radiometric measurements) with probabilistic a priori information (e.g., stratigraphic ordering of archaeological and/or sedimentary levels) observed at an archaeological site. When Bayesian age modeling methods are applied to an archaeological context, the age measurements (e.g.,  $^{14}\text{C}$ ) serve to improve, via the properties of conditional probability, a priori information such that one obtains a result that serves to improve the understanding of the timing and duration of associated archaeological events. The  $^{14}\text{C}$  measurements produced in the framework of this study and those recently published and pertaining to the target Upper Paleolithic archaeological typo-technological complexes are integrated into two hierarchical Bayesian age models using the ChronoModel software package [58,62] and the intersecting multiphase approach and chronological data described by Banks et al. [1].

One advantage of ChronoModel over other available and commonly used software packages is its use of the Event date concept. This parameter represents the unknown calendar date of a temporal event within a given chronology. Assuming that the Event can be associated with one or more suitable samples from which an age or age measurements have been obtained, the Event model combines these calendar dates in order to estimate the Event's unknown target date. It is important to point out that each unique sample, whether it yielded one or more age estimates (e.g., multiple measurements obtained from a single sample), is assumed to represent a unique event. Each archaeological level represents a palimpsest of an unknown number of events and is defined as a phase in ChronoModel. A phase is a group of archaeological events, represented by event dates, that one wishes to situate chronologically. Due to the fact that it is difficult to determine with certainty the rhythm with which events occurred through time, ChronoModel assumes that a phase's event dates are uniformly distributed within it and that the temporal boundaries of the chronological framework are defined by the start and end times of the broad 'study period' [60]. ChronoModel allows one to estimate the beginning, duration, and termination of a phase based on the posterior event dates observed within it. This represents a significant departure from and improvement over approaches that rely on the Naylor–Smith–Buck–Christen (NSBC) prior [53–56]. For software packages that rely on this prior [57,63,64], it

is applied to a group of dates placed within a phase that is situated between two hyper-parameters (start and end) in the Bayesian hierarchical structure. Within a phase, dates are assumed to be conditionally independent from these two boundaries and uniformly distributed between them. Via the subsequently assigned uniform prior joint density, the NSBC prior elicits an effect such that dates move closer to one another a posteriori [58]. ChronoModel's use of the Event model and its application of start (Ta) and end (Tb) temporal boundaries to the broader so-called 'study period' prevent the temporal compression observed in other commonly used Bayesian modeling software packages.

The intersecting multiphase approach that we employ consists of constructing an individual phase model for each stratified archaeological sequence under consideration, in which each archaeological level is a phase that contains event models each populated with the individual  $^{14}\text{C}$  measurements from archaeological samples associated with that level. Simultaneously, these same event models, along with those from single-component (i.e., non-stratified) archaeological contexts, are placed within a separate phase model in which each phase represents a recognized archaeological culture (i.e., cultural taxonomic unit: e.g., Recent Gravettian, Final Gravettian, etc.), such that a "cultural" phase may contain multiple events derived from a number of archaeological levels from one or more sites. This intersecting structure allows ChronoModel to take into account the stratigraphic priors associated with each event along with the priors related to the succession of archaeological cultures observed in a regional archaeological cultural trajectory when calculating the age intervals for successive or contemporaneous archaeological cultures. This structure is advantageous in constructing regional cultural chronologies because it avoids the statistically undesirable practice of breaking the Bayesian scheme into two separate steps, a statistically undesirable practice that is required with OxCal in which a second-generation model is populated with a posteriori probability distributions derived from first-generation age models of individual stratified archaeological sequences [60,61].

We employ two hierarchical Bayesian age-model structures to examine the regional chronology of archaeological taxonomic units. The first is the same intersecting, multiphase structure published previously [1]. First, we run this model, which was produced with IntCal13, using the same data published in 2019 and the IntCal20 calibration curve [65]. Next, using the same model and original data, we inject the radiocarbon measurements obtained in the framework of this study, as well as those published recently. In this model structure, the time period that is of particular interest to us, the Middle Gravettian, is divided into two parallel typo-technological phases: The Pyrenees Middle Gravettian and the northern generic Middle Gravettian. The latter groups together  $^{14}\text{C}$  measurements from archaeological levels that are either Noaillian, Rayssian, or contain lithic diagnostics of both. The purpose of re-running this same model structure with the most recent calibration curve, as well as with newly published  $^{14}\text{C}$  ages along with those that we produced, is to evaluate how the newly calculated age intervals compare to those published in 2019. In order to be consistent with the modeling process employed by Banks et al. [1], after the initial runs, chronometric measurements with a Markov posterior standard deviation greater than 400 were considered to be outliers. These radiometric measurements were removed from the model before running it a second time. It is the results of this second model run that we present.

For the second age model, we maintain an intersecting multiphase structure in which the phases are archaeological levels and the stratigraphic relationships for individual sites or archaeological sequences, as described by Banks et al. [1] (Figure 1) make up one component of the structure. The sites that compose this portion of the intersection, multiphase model are Le Blot, Carane, Casserole, Cuzoul de Vers, Flageolet I, Fontgrasse, Gargas, Laugerie Haute oust, Ormesson, Pataud, Petit Cloup-Barat, Peyrugues, St. Aubin, Talillis des Coteaux, and Tarté (see Table S1 for details concerning their individual archaeological levels). This component intersects with a separate cultural phase portion (Figure 3) in which we organize the Middle Gravettian in the following manner: a Pyrenees Middle Gravettian phase situated between the geographically broader Early Gravettian and the Recent

Gravettian. We differentiate the Pyrenees Middle Gravettian from the Middle Gravettian in contexts north of the Garonne River valley since, within the latter, we observe a stratigraphic succession from the Noaillian phase to the Rayssian phase—a pattern not observed in regions south of the Garonne. Therefore, parallel to the Pyrenees Middle Gravettian phase (i.e., between the Early and Recent Gravettian phases) are two successive phases, the Northern Noaillian and the Rayssian, with the former preceding the latter. Finally, we establish a parallel Northern mixed Middle Gravettian phase for the single archaeological level that cannot be attributed to either the Noaillian or the Rayssian unequivocally (i.e., Pataud level 4 middle).

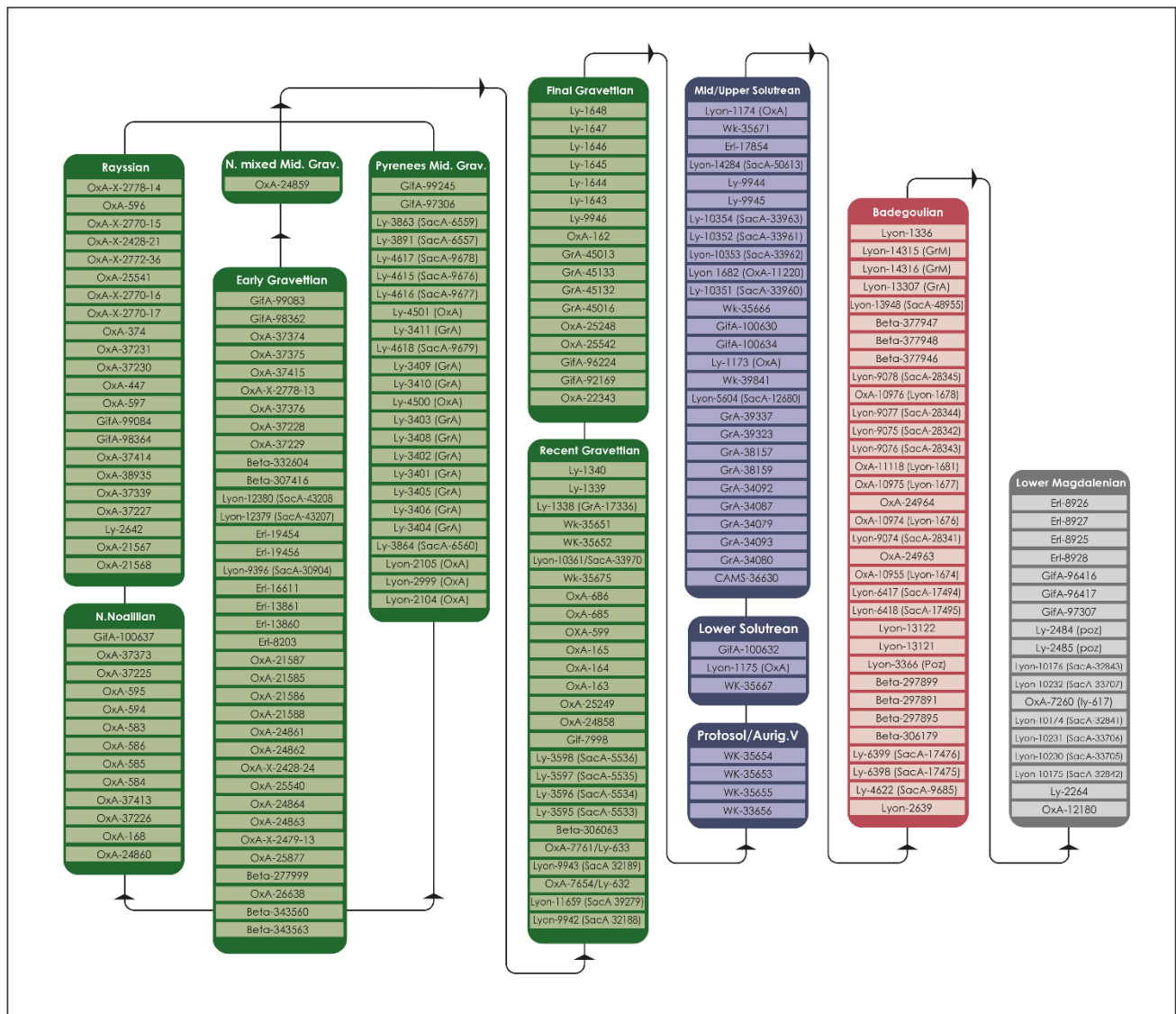


**Figure 3.** Depiction of the stratigraphic or chronological succession of archaeological (typo-technological) cultural phases that make up the cultural phase portion of the intersecting phase structure of the age model constructed in ChronoModel. In this portion of the age model, the Northern Noaillian (N. Noaillian) and Rayssian phases of the Middle Gravettian are successive, with the Northern Noaillian preceding the Rayssian. These two successive phases are parallel to the Northern mixed Middle Gravettian (N. mixed Mid. Grav.) and Pyrenees Middle Gravettian (Pyrenees Mid. Grav.) phases. All of these Middle Gravettian phases are preceded by the Early Gravettian and followed by the Recent Gravettian. The remainder of the archaeological cultural phases and their chronological relationships are identical to a previously employed model structure [1].

The reason for creating two successive phases for the Noaillian and Rayssian in regions north of the Pyrenees is that it follows an existing hypothesis founded on a number of elements. Based on various examinations of archaeological data, Banks et al. [1] and Klaric et al. [17] postulate that in northern Aquitaine (France) and regions further north, the Rayssian post-dates the Noaillian. Thus, it would logically have occurred during Greenland Stadial (GS) 5.1, during which Heinrich Event (HE) 3 occurred. This postulate is supported by several observations. First, in stratified archaeological sequences that contain a continuous cultural record for the Gravettian, the Noaillian is present immediately following the Lower Gravettian [6,16,23]. Unfortunately, the majority of archaeological sequences (i.e., stratified sites) in areas north of the Garonne River are taphonomically complex and their Middle Gravettian levels contain diagnostic Noaillian and Rayssian lithic artifacts to varying degrees. The pattern observed at the Pataud rockshelter, which is the only existing reference with stratified levels of high quality, is that in the lower Middle Gravettian levels, Noaillian diagnostic artifacts (i.e., Noailles burins) are predominant with only rare Rayssian elements (e.g., the lower subdivision of Pataud level 4). This trend is reversed as one moves up the stratified sequence, such that lithic assemblages from younger Middle Gravettian levels are predominantly Rayssian in character with occasional Noaillian burins or pseudo Noaillian burins (e.g., the upper subdivision of Pataud level 4). Such a pattern is to be expected by a Noaillian–Rayssian succession in sites that have been affected by post-depositional processes. Second, there is a clear technical rupture between Rayssian and Noaillian lithic industries [16,17,23]. This rupture, in conjunction with the fact that most stratified sequences that contain the two have been affected by post-depositional processes, serves to weaken arguments that Noaillian and Rayssian lithic assemblages are contemporaneous and represent functional differences [35,66] in northern areas of the Nouvelle Aquitaine Region. Third, taking into consideration other elements of Middle Gravettian material culture, one observes during the Rayssian that technical methods to produce rods (*baguettes* in French) from reindeer antler and ivory that served as blanks for the manufacture of formal tools, predominantly the tips of hunting weapons, are more diverse than those used during the Noaillian or Lower Gravettian and are identical to the panoply of rod extraction methods present during the Recent Gravettian [17], a pattern suggesting a cultural relation between the Rayssian and the Recent Gravettian. Last, Klaric et al. [17] point out that faunal remains recovered from Rayssian archaeological contexts are dominated by reindeer and to a lesser extent horse, species that are arctic and steppic, respectively, and that would have been predominant during the latter stages of GS 5.1.

All of the Middle Gravettian archaeological levels and their archaeological culture attributions for the second age model are indicated in Table S1. These attributions are based on the evaluations of lithic assemblages carried out by Vignoles [6] on the sites of Les Jambes, Le Facteur, and Le Flageolet I which are summarized in the site descriptions above. Our attributions of the levels from the Pataud rockshelter are based on evaluations of the site's Gravettian level lithic assemblages by one of us (L.K.), and the same holds true for the attributions for the site of Callan (A.M.) [40].

While we remove outliers from the runs of the original model in order to remain consistent with the previous approach [1], we do not do this for the second model structure that contains individual phases for the Noaillian and Rayssian. The reason is that the event date model employed in ChronoModel automatically penalizes chronometric measurements whose calibrated dates are far from the target event date or in contradiction with stratigraphy. This penalization eliminates the need for a dedicated outlier detection method [59]. The reason for removing outliers in the previous study was to test the efficacy of the automatic outlier penalization, and the comparison between initial model results to those for which outliers had been removed showed that the results of the two were essentially identical [1]. Therefore, we deem this supplementary analytical step unnecessary.

With respect to ChronoModel configurations, we employ the “Age Cal. BP” time scale setting with a study period defined as 35–14 cal ka BP. We also use the default MCMC



settings: 3 chains, 1000 burn iterations, 500 batch iterations with a maximum of 20 batches, and 100,000 acquisition iterations with a thinning interval of 10 [62].

### 3. Results

#### 3.1. Radiocarbon Measurement Results

Out of the 32 faunal remains and two charcoal samples submitted for radiocarbon dating, 10 faunal remains were withdrawn following %N screening since their values ( $\leq 0.38$  %N) suggested that the chances of obtaining a date were poor. Out of the 24 maintained samples, three failed, resulting in a total of 23  $^{14}\text{C}$  measurements (Table 2) from 21 samples—two faunal samples (Flageolet-3 and Flageolet-12) were dated twice. Out of the 20 dated faunal remains, age measurements for five were obtained from ultrafiltered collagen samples, and the rest were measured from non-ultrafiltered collagen samples.

The only aberrant measurement is from the viable charcoal sample from La Picardie, which is Holocene in age. Our ages from Le Flageolet I levels VII and VI, which we attribute to the Lower Gravettian, correspond well to a number of ages obtained from the level attributed to the same cultural phase at the Pataud rockshelter (various lenses in level 5) [37,67] (Table S1). Likewise, our ages for le Flageolet I levels V and IV, which we attribute to the Rayssian, correspond well to one of the ages from level V published by Rigaud et al. [27], as well as a number of the ages associated with level 4 upper at the Pataud rockshelter [37]. The same is true for our ages obtained from Les Jambes, in that they are comparable to those from Pataud level 4 upper. We do see inconsistencies, however, between our ages from Le Callan and Le Facteur, whose dated levels we attribute to the Noaillian, and those from the Noaillian level (4 upper) at Pataud. Our results from these two contexts are younger than what we expected to obtain for Noaillian occupations. With this dating campaign, we have added a large number of radiocarbon measurements to the existing population of ages associated with Gravettian contexts in southwestern France. In addition, it is important to have produced  $^{14}\text{C}$  ages for the site of Les Jambes, a site that until now had not been the subject of chronological analyses.

#### 3.2. Age Model Results

As described above, we ran a number of Bayesian age models. The first was the exact same model and radiocarbon data published previously [1], re-run here with the IntCal20 curve. The second age model used the same nested structure as the one published previously. We injected our new radiocarbon ages into it and excluded ages that could be considered outliers based on their posterior standard deviation values. Finally, for the third age model, we modified the cultural phase portion of the model structure so that it included two successive typo-technological phases, the Northern Noaillian and the Rayssian, that were situated parallel to a contemporaneous phase for the Middle Gravettian Noaillian assemblages from the Pyrenees (i.e., areas south of the Garonne River). Into this model, we fed all of the radiocarbon ages employed in the 2019 study, those published by others since 2019, as well as those produced in the framework of this study.

The IntCal20 calibrated intervals and posterior event date Highest Posterior Density (HPD) for all  $^{14}\text{C}$  measurements are presented in Table S1, and the modeled chronological intervals (95%) for each model's cultural (typo-technological) phases are contained in Table 3.

**Table 2.** Uncalibrated  $^{14}\text{C}$  measurements obtained from faunal and charcoal remains from Gravettian age site levels. Also provided are their taxonomic identifications, C and N isotopic values, and percent collagen yields. Pretreatment codes (Pcode): AG—gelatin sample, AF—ultrafiltered collagen (gelatin), ZR—acid-base-acid. Table available at <https://doi.org/10.48579/PRO/UIGKGW>.

| Site           | Level             | Unit/Square | Sample ID               | Pcode | Lab Code        | Age    | Error | $\delta^{13}\text{C}$ | $\delta^{15}\text{N}$ | %colY | Genus/Species            | Human Modification                 |
|----------------|-------------------|-------------|-------------------------|-------|-----------------|--------|-------|-----------------------|-----------------------|-------|--------------------------|------------------------------------|
| Le Callan      | c. I-II           | H4          | Callan-3                | AG    | OxA-37373       | 25,590 | 250   | −19.5                 | 6.1                   | 1.3   | <i>Rangifer tarandus</i> | Cutmarks                           |
| Le Callan      | c. I-II           | G4          | Callan-4                | AG    | OxA-37225       | 25,020 | 220   | −19.6                 | 6.6                   | 1.3   | <i>Rangifer tarandus</i> | green bone break                   |
| Le Facteur     | Chantier J, c. 11 | sondage 72  | Facteur-2               | AF    | OxA-37413       | 24,740 | 190   | −19.9                 | 6.8                   | 3.6   | <i>Rangifer tarandus</i> | scraping; green bone break         |
| Le Facteur     | Chantier J, c. 11 | sondage 72  | Facteur-3               | AG    | OxA-37226       | 25,190 | 230   | −19.9                 | 7.4                   | 2     | <i>Rangifer tarandus</i> | green bone break; possible cutmark |
| Le Flageolet I | c. VII            | C9          | Flageolet-1             | AG    | OxA-37374       | 27,630 | 330   | −19.1                 | 7.2                   | 2.2   | <i>Cervus elaphus</i>    | scraping                           |
| Le Flageolet I | c. VII            | C10         | Flageolet-3             | AG    | OxA-37375       | 28,250 | 330   | −20.1                 | 5                     | 2.3   | Bovidae                  | cutmarks                           |
| Le Flageolet I | c. VII            | C10         | Flageolet-3: duplicate  | AF    | OxA-37415       | 28,110 | 280   | −20                   | 5.1                   | 1.2   | Bovidae                  | cutmarks                           |
| Le Flageolet I | c. VI             | C8          | Flageolet-5             | AG    | OxA-X-2778-13 * | 27,850 | 700   | −20.3                 | 5.3                   | 0.2   | size IV                  | cutmarks                           |
| Le Flageolet I | c. VI             | C7          | Flageolet-6             | AG    | OxA-37376       | 27,560 | 300   | −20.2                 | 4.9                   | 0.8   | Bovidae                  | cutmarks                           |
| Le Flageolet I | c. VI             | C7          | Flageolet-7             | AG    | OxA-37228       | 25,870 | 250   | −19.6                 | 6.3                   | 2.5   | <i>Rangifer tarandus</i> | cutmarks                           |
| Le Flageolet I | c. VI             | C7          | Flageolet-8             | AG    | OxA-37229       | 27,460 | 300   | −19.9                 | 4.3                   | 1.8   | <i>Rangifer tarandus</i> | cutmarks                           |
| Le Flageolet I | c. V              | C10         | Flageolet-10            | AG    | OxA-37230       | 26,110 | 250   | −20.8                 | 6.3                   | 1.2   | <i>Equus sp.</i>         | retoucher                          |
| Le Flageolet I | c. V              | C10         | Flageolet-11            | AG    | OxA-37231       | 26,230 | 260   | −19.5                 | 6.4                   | 1.4   | <i>Rangifer tarandus</i> | none                               |
| Le Flageolet I | c. V              | C9          | Flageolet-12            | AG    | OxA-X-2770-16   | 26,000 | 260   | −19                   | 7.9                   | 0.9   | <i>Rangifer tarandus</i> | cutmarks                           |
| Le Flageolet I | c. V              | C9          | Flageolet-12: duplicate | AG    | OxA-X-2770-17   | 26,710 | 300   | −18.8                 | 7.7                   | 0.6   | <i>Rangifer tarandus</i> | cutmarks                           |
| Le Flageolet I | c. V              | C9          | Flageolet-13            | AG    | OxA-X-2772-36   | 25,900 | 500   | −19.1                 | 6.5                   | 0.2   | <i>Rangifer tarandus</i> | scraping                           |
| Le Flageolet I | c. V              | C10         | Flageolet-14            | AG    | OxA-X-2770-15   | 26,630 | 280   | −18.4                 | 6.6                   | 0.8   | <i>Rangifer tarandus</i> | cutmarks; scraping                 |
| Le Flageolet I | c. IV             | C6          | Flageolet-21            | AG    | OxA-X-2778-14 * | 25,700 | 450   | −19.2                 | 7                     | 0.2   | <i>Rangifer tarandus</i> | cutmarks                           |
| Les Jambes     | c. 3              | B0          | Jambes-1                | AG    | OxA-37227       | 26,060 | 250   | −20.6                 | 5                     | 2.8   | <i>Equus sp.</i>         | none                               |
| Les Jambes     | c. 3              | B           | Jambes-2                | AF    | OxA-37414       | 25,450 | 200   | −19.1                 | 6.4                   | 1.9   | <i>Rangifer tarandus</i> | none                               |
| Les Jambes     | c. 2              |             | Jambes-4                | AF    | OxA-37339       | 25,790 | 210   | −20                   | 7.2                   | 2.4   | <i>Equus sp. (?)</i>     | none                               |
| Les Jambes     | c. 3              | B           | Jambes-5                | AF    | OxA-38935       | 25,180 | 190   | −19.5                 | 5.6                   | 2.7   | <i>Rangifer tarandus</i> | possible digestion                 |
| La Picardie    | c. 2na1           | G10A        | Picardie-4              | ZR    | OxA-41188       | 6621   | 21    | −27.35                | n/a                   | n/a   | <i>Quercus</i>           |                                    |

\* very small graphite target.

**Table 3.** Modeled intervals (calibrated calendar years BP) for typo-technological phases in the cultural phase component of the various age models. Table also available at <https://doi.org/10.48579/PRO/ATD1RD>.

| Typo-Technological Phase                | 2nd Generation Model [1]<br>IntCal13<br>Modeled Interval (95%) |          |                | 2nd Gen. Model [1]<br>Minus Outliers;<br>IntCal20<br>Modeled Interval (95%) |          |                | 2019 Model Structure<br>with<br>New Ages, Minus<br>Outliers; IntCal20<br>Modeled Interval (95%) |          |                |
|---|--|----------|----------------|---|----------|----------------|---|----------|----------------|
|   | Begin  | End      | duration (yrs) | Begin   | End      | duration (yrs) | Begin   | End      | duration (yrs) |
| Lower Magdalenian *                     | 21,182   | 17,978 * | —              | 21,211  | 17,988 * | —              | 21,195  | 17,985 * | —              |
| Badegoulian                             | 23,090   | 20,777   | 2313           | 23,092  | 20,792   | 2300           | 23,117  | 20,799   | 2318           |
| Middle & Upper Solutrean                | 24,470   | 22,787   | 1683           | 24,440  | 22,836   | 1604           | 24,433  | 22,880   | 1553           |
| Lower Solutrean                         | 25,402   | 24,007   | 1395           | 25,387  | 23,951   | 1436           | 25,391  | 23,952   | 1439           |
| Aurignacian V/Protosolutrean            | 26,173   | 25,371   | 802            | 26,202  | 25,367   | 835            | 26,179  | 25,355   | 824            |
| Final Gravettian                        | 27,126   | 25,810   | 1316           | 27,140  | 25,836   | 1304           | 27,145  | 25,811   | 1334           |
| Recent Gravettian                       | 28,973   | 26,655   | 2318           | 29,165  | 26,670   | 2495           | 29,093  | 26,701   | 2392           |
| Middle Gravettian (north of Pyrenees)   | 31,520   | 28,589   | 2931           | 31,688  | 28,788   | 2900           | 31,135  | 28,743   | 2392           |
| Middle Gravettian Pyrenees              | 31,925   | 28,614   | 3311           | 32,116  | 28,821   | 3295           | 31,158  | 28,828   | 2330           |
| Early Gravettian *                      | 34,990 *   | 31,245   | —              | 35,301 *  | 31,388   | —              | 36,049*   | 30,753   | —              |
| <b>Model w/new ages<br/>IntCal20</b>    |  |          |                |   |          |                |   |          |                |
| <b>Modeled Interval (95%)</b>           |  |          |                |   |          |                |   |          |                |
| Typo-Technological Phase                |  |          |                |   |          |                | Begin   | End      | duration (yrs) |
| Lower Magdalenian *                     |  |          |                |   |          |                | 21,158  | 18,499 * |                |
| Badegoulian                             |  |          |                |   |          |                | 23,119  | 20,798   | 2321           |
| Middle & Upper Solutrean                |  |          |                |   |          |                | 24,439  | 22,893   | 1546           |
| Lower Solutrean                         |  |          |                |   |          |                | 25,382  | 23,964   | 1418           |
| Aurignacian V/Protosolutrean            |  |          |                |   |          |                | 26,143  | 25,306   | 837            |
| Final Gravettian                        |  |          |                |   |          |                | 27,064  | 25,725   | 1339           |
| Recent Gravettian                       |  |          |                |   |          |                | 29,036  | 26,580   | 2456           |
| Rayssian                                |  |          |                |   |          |                | 30,519  | 28,518   | 2001           |
| Northern Noaillain                      |  |          |                |   |          |                | 31,205  | 29,995   | 1210           |
| Middle Gravettian (north of Pyrenees) * |  |          |                |   |          |                | 30,797 *  | 29,916 * | 881            |
| Pyrenees Middle Gravettian (Noaillain)  |  |          |                |   |          |                | 31,233  | 28,600   | 2633           |
| Early Gravettian *                      |  |          |                |   |          |                | 36,446 *  | 30,809   |                |

\*—The beginning of the Early Gravettian and the end of the Lower Magdalenian are in italics and marked with an asterisk because these two typo-technological phases were populated with a non-exhaustive sample of radiocarbon measurements in order to reliably constrain the cultural phases targeted in this study. The same is true for the Generic Middle Gravettian (north of Pyrenees) phase in the model structure with the successive Noaillain and Rayssian phases due to the fact that this phase contained only a single radiocarbon age; therefore, its calculated duration is not robust.

The cultural phase chronological intervals of the published 2019 model, originally calculated using IntCal13, differ very little from those obtained by rerunning the same model with the newest calibration curve, IntCal20. The same pattern is largely the case when the

2019 model run with IntCal20 is compared to the model using the same radiocarbon data and model structure published in 2019, into which we injected the new radiocarbon dates that we obtained in the framework of this study, in addition to those published since 2019. For cultural phases posterior to the Middle Gravettian, one observes that the posterior modeled age intervals for the different phases only differ by a few to several decades. Larger differences, though, are apparent between the two models with respect to the Early Gravettian and the two broad Middle Gravettian phases. In the model that incorporates the newest ages, the Early Gravettian terminates a few hundred years more recently, around ca. 31 cal ka BP. The northern Middle Gravettian phase has a slightly shorter duration due to the fact that the beginning of its chronological interval occurs approximately 300 years more recently than the 2019 model that uses the IntCal20 curve. It, however, still falls within the span of time covered by the latter half of GS-5.2, through GI-5.1 and GS-5.1, with a termination in the initial stages of GI-4. The biggest difference between the two models is observed for the Pyrenees Middle Gravettian phase. In the newer model, this phase has a shorter chronological interval of approximately 600 years, and this is because the latter limit of the Lower Gravettian is younger, causing the Pyrenees Middle Gravettian to begin after the onset of GS-5.2. This is in contrast to the interval modeled without the newest dates, for which it begins during the preceding GI-5.2. In the new model, the Pyrenees Middle Gravettian interval terminates during GI-4.

Concerning the model with successive typo-technological phases for Northern Noaillian and Rayssian archaeological contexts, we observe that these phases have modeled durations of roughly 1200 and 2000 years, respectively (Table 3). The Northern Noaillian phase begins at roughly 31.2 cal ka BP during the latter half of GS-5.2, which is roughly the same as is observed in the preceding model in which these contexts were contained in a single, broad phase. The Northern Noaillian terminates around 29.9 cal ka BP, which is towards the beginning of HE3 (Figure 4). The beginning of the HPD for the Rayssian phase occurs around 30.5 cal ka BP, just prior to the onset of GS-5.1, and its other extreme is situated near the termination of GI-4, around 28.5 cal ka BP. The overlap between the peaks of Northern Noaillian's terminal HPD and the Rayssian's initial HPD is situated during the early stages of GS-5.1, and the peak of the Rayssian's terminal HPD falls at the midpoint of GI-4. This model structure indicates that the technical features associated with the Rayssian are primarily concomitant with stadial climatic conditions and occur within the timeframe of HE3. Finally, the model indicates that the transition between the Rayssian and the Recent Gravettian occurred during GI-4.

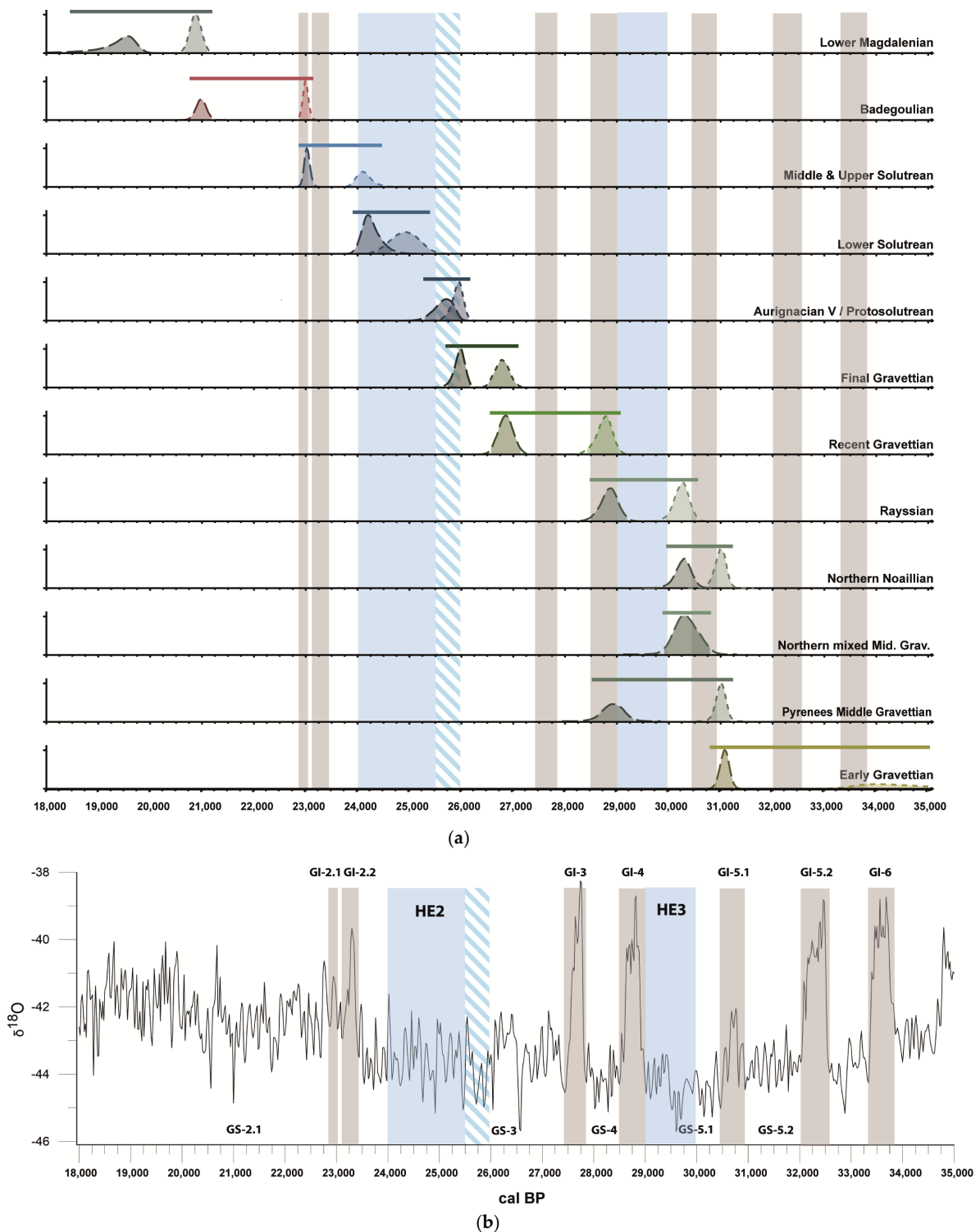


**Figure 4.** Phase interval results for each typotechnological (cultural) phase produced in the age model structure in which specific and successive phases were included for the Noaillian and Raysian phases in regions north of the Pyrenees. (a) Modeled chronological intervals for the examined typotechnological phases. The solid bars depict the shortest intervals within which fall the beginning and end of each phase at the 95% confidence level. Highest posterior density distributions (95%) for the beginning (dotted) and end (dashed) of each cultural phase are also illustrated. (b) NGRIP  $\delta^{18}O$  record [68]. The chronological intervals for Heinrich Events (HE) 3 and 2 are depicted in blue. The color-dashed interval preceding HE2 represents a period of North Atlantic cooling [69]. Greenland Interstadials (GI) are depicted in grey.

#### 4. Discussion

The two age models containing new radiocarbon data presented in this study confirm that the Middle Gravettian falls within a chronological window, 31.2–28.5 cal ka BP, that encompasses Greenland Interstadial 5.1 and Greenland Stadial 5.1. In Western Europe, this interval is a period during which a trend towards an opening of the landscape with respect to vegetation is observed [70,71], even in southern alpine foothill contexts [72], a trend replicated with dynamic global vegetation models [73]. This pattern is paired with an increase in the frequency of loess deposition and periglacial features [74–77].

In both the Pyrenees and regions to the north, archaeological assemblages containing Noailles burins appear towards the end of GS-5.2. While the factors implicated in the appearance of the Noaillian remain to be identified, its appearance towards the end of a stadial phase would suggest that its genesis reflects more the influence of cultural factors than environmental ones, and if the latter were implicated, it would seem to be to a lesser degree. As stated above, our reading of the Middle Gravettian archaeological record leads us to propose the hypothesis that the Rayssian post-dates the Noaillian in regions north of the Garonne River. The output of our model, with a cultural phase structure reflecting this relationship, places the appearance of contexts containing assemblages associated with the Rayssian lithic technical system during the terminal portion of GI-5.1, and it is present throughout GS-5.1 (which includes Heinrich Event 3) and into the climatic amelioration of GI-4. Despite the Rayssian's initial appearance during a brief and relatively weak interstadial phase, its duration suggests that its lithic technology was compatible with the environmental conditions of Greenland Stadial 5.1, and this compatibility could explain its relative longevity.

The Rayssian lithic technical system is recognizable by its method of producing highly standardized bladelets to be used as elements in hunting weapon tips. The highly standardized system of lithic reduction used to produce Picardie bladelets was also flexible in the sense that diverse blanks (e.g., thick flakes or blades, or fragments of such) could be used to create the characteristic Rayssian cores used to produce such bladelets. This flexibility and ability to quickly produce standardized hunting weaponry elements falls within the definition of a maintainable system [78]. Such systems are typical of highly mobile hunter-gatherer groups, including those whose subsistence system is focused on the intercept hunting of migratory prey species during certain periods of the year. The reason is that access to high-quality lithic raw materials needed to repair hunting weapons cannot be fully predicted during prolonged periods of intercept hunting. The use of a flexible system of core production and management provides the ability to use transported lithic raw materials to manufacture lithic hunting weapon elements to replace those that were broken or lost during use, and in areas where access to lithic raw material sources was potentially limited or non-existent. Maintainability can be paired with the concept of curation, with the latter being a measure of how much utility was extracted from a tool, with reference to its maximum utility, prior to discard [79]. An analysis of Rayssian bladelet cores from two sites, one close to quality lithic raw material sources and the other not, demonstrates that Rayssian burin-cores were heavily curated in the lithic-poor region [80]. These maintainability and curation characteristics of the Rayssian lithic system, or at least components of it directly linked to hunting activities, fit well with expectations for mobile hunter-gatherer groups in cold, open environments that would have contained a non-diverse spectrum of highly mobile prey. Such is the case for the Rayssian, whose contexts are dominated by reindeer remains [17,81]. This signature of subsistence specialization and related technical innovations during the Rayssian is also reflected in analyses of the ecological niche exploited by groups during this cultural phase. Vignoles [6] finds that the Rayssian ecological niche, with respect to the Noaillian niche (both north of the Garonne and for the Noaillian as a whole), contracts and is focused on a very specific set of environmental conditions. Thus, its specialized production of hunting armatures appears to directly reflect this focus on a relatively narrow ecological niche.

This trend towards a differentiation due to specialization already existed to a certain degree between Pyrenees Noaillian contexts and those situated north of the Garonne River, with the latter being specialized in reindeer hunting and the former associated with the exploitation of a more diverse spectrum of prey species [81,82].

Finally, both the Rayssian and the Pyrenees Noaillian terminate at the onset of or during GI-4, and the subsequent appearance of the Recent Gravettian suggests that the technological features observed with this latter phase were well-suited to the environmental conditions of the roughly 500-year time period following Heinrich Event 3. It has been proposed that the disappearance of the highly normative Raysse method for producing hunting weaponry and the subsequent appearance of a more flexible method of making backed lithic inserts for composite hunting weapons are likely related to human territorial modifications resulting from environmental and resource reorganizations brought about by the rapid and relatively marked climatic changes of the GS-5.1–GI-4 transition [6]. It is probable that the Recent Gravettian lithic system was derived from Raysse burin-core technology but accepted a wider range of variation in the lithic knapping process. We hypothesize that this is related to changes in social transmission processes or the consequence of less strict and more easily transmissible and maintainable cultural adaptations during the Recent Gravettian as a result of the proposed territorial and mobility transformations. This cultural transition between the Middle and Recent Gravettian was likely staggered, with an appearance first in southern regions followed by a slightly later appearance in higher latitudes. For example, Paris [83] describes radiocarbon measurements from the site of Renancourt 1 (Northern France) that indicate Recent Gravettian occupations beginning there as of GI-3, ca. 28 ka cal BP, which is several centuries after the transition indicated by our age model (Figure 4). Such delays in the settlement of higher latitude regions in our study area have been previously proposed [83,84] and are an expected pattern when human groups begin using previously uninhabited regions [85].

With respect to this study's objectives, we have added a number of new radiocarbon ages from Gravettian contexts to the available corpus of chronological data. Unfortunately, our expectation that newly obtained radiocarbon ages from the targeted sampling of specific archaeological contexts would unequivocally improve our understanding of the Rayssian's chronological extension was not entirely met. For example, the  $^{14}\text{C}$  measurements obtained from the site of Callan are younger than we expected for a purely Noaillian context, which we propose precedes the Rayssian, as they overlap almost entirely with GS-5.1 when simply calibrated and do not overlap (or at least minimally with respect to OxA-37373) with the posterior interval obtained for the Northern Noaillian in our model that separates the Noaillian and Rayssian into successive phases. The same holds true for the site of Le Facteur, as our new ages are relatively young for what we interpret to be predominantly a Noaillian assemblage. On the other hand, for the site of Les Jambes, which we interpret to represent Rayssian occupations, the ages that we obtained, with the exception of one (OxA-37227), fall within GS-5.1 when calibrated. We were unable to date the purely Rayssian open-air archaeological context of La Picardie as one of our charcoal samples failed to produce an age and the other represents intrusive, Holocene-age charcoal. La Picardie effectively illustrates the difficulties that we face in trying to obtain chronological data from open-air Rayssian contexts in which organics are rarely or poorly preserved (e.g., La Picardie, Solvieux) and also serves as an excellent example of our difficulty in grasping the chronology of Middle Gravettian contexts situated in regions north of the Loire River. It is also important to keep in mind the fact that we are attempting to evaluate the chronology of two typo-technocomplexes that are defined differently—the Noaillian by the presence of a particular type of burin and the Rayssian by a specific and recognizable lithic reduction technique for producing bladelets—and this use of criteria that are not necessarily comparable renders our understanding of the chronological relationship difficult.

However, based on our reading of the Middle Gravettian archaeological record and our Bayesian age model structure that operationalizes our interpreted relationship between the Noaillian and the Rayssian typo-technocomplexes, we propose that the Noaillian north

of the Garonne River appears slightly after Noaillian contexts observed in the Pyrenees, both during GS-5.2. Our model indicates that the Rayssian, based on the few dated contexts available, appears during the termination of the relatively minor Greenland Interstadial 5.1 and covers the entirety of GS-5.1. Thus, it appears to represent a technology well-suited to the environmental conditions of GS-5.1, during which we observe Heinrich Event 3. Naturally, our chronological evaluation of the relationship between the Noaillian and Rayssian is grounded on specific hypotheses, and our findings will need to be evaluated further as new archaeological and chronological data become available.

**Supplementary Materials:** The following supporting information can be downloaded at: <https://doi.org/10.48579/PRO/ATD1RD>. Table S1: List of  $^{14}\text{C}$  ages, and their associated archaeological contexts, analyzed with the two Bayesian age model structures described in the text. The ages are organized by archaeological cultural phase. The unmodeled (calibrated) Highest Posterior Distributions (HPD, 95%) are provided in columns H and I. Columns J and K contain the results of Banks et al.'s [1] model run with the IntCal20 calibration curve [65]. Columns L and M contain the posterior intervals for event dates and cultural phases obtained by employing the same model structure as Banks et al. [1], including newly published ages as well as those obtained in this study. Columns N and O present posterior intervals for event dates and cultural phases obtained with an age model that separates the Northern Noaillian and Rayssian cultures of the Middle Gravettian into distinct, successive phases. Outlier determinations were made by examining the median (Q2) posterior standard deviations for the individual event dates; those with values greater than 420 are considered outliers. Outliers were removed from the models by employing the 2019 model structure. Since outliers are heavily penalized by ChronoModel, their removal was not necessary for the second model structure that separated the Northern Noaillian and Rayssian into successive phases. Event dates with median posterior standard deviations greater than 420 are depicted in bold, maroon italics in columns N and O [86–121].

**Author Contributions:** Conceptualization, W.E.B., A.V., and L.K.; methodology, W.E.B.; formal analysis, W.E.B.; investigation, W.E.B., A.V., J.L., A.M., and L.K.; resources, W.E.B.; data curation, W.E.B.; writing—original draft, W.E.B., A.V., and L.K.; writing—review and editing, W.E.B., A.V., J.L., A.M., and L.K.; visualization, W.E.B. and A.V.; supervision, W.E.B. and L.K.; project administration, W.E.B.; funding acquisition, W.E.B. and L.K. All authors have read and agreed to the published version of the manuscript.

**Funding:** This study was funded by the Conseil Régional Aquitaine (2018-1R40205).

**Data Availability Statement:** Data pertaining to the archaeological samples selected for the described radiocarbon dating and subsequent radiocarbon results are available at <https://doi.org/10.48579/PRO/U1GKGW>. The results of the hierarchical Bayesian age models are available at <https://doi.org/10.48579/PRO/ATD1RD>.

**Acknowledgments:** The research described here benefited from the scientific framework of the University of Bordeaux's IdEx "Investments for the Future" program/GPR "Human Past". We warmly thank Jean-Philippe Rigaud who kindly offered his excavation notes and expertise related to the site of Le Flageolet I and participated in the selection of faunal remains to be radiocarbon dated. His expertise and advice were of great utility. Finally, we thank Gauthier Devilder for preparing Figures 3 and 4.

**Conflicts of Interest:** The authors declare no conflicts of interest. The funders had no role in the design of the study; in the collection, analyses, or interpretation of data; in the writing of the manuscript; or in the decision to publish the results.

## References

1. Banks, W.E.; Bertran, P.; Ducasse, S.; Klaric, L.; Lanos, P.; Renard, C.; Mesa, M. An Application of Hierarchical Bayesian Modeling to Better Constrain the Chronologies of Upper Paleolithic Archaeological Cultures in France between ca. 32,000–21,000 Calibrated Years before Present. *Quat. Sci. Rev.* **2019**, *220*, 188–214. [[CrossRef](#)]
2. Binford, L.R. *Constructing Frames of Reference: An Analytical Method for Archaeological Theory Building Using Ethnographic and Environmental Data Sets*; University of California Press: Berkeley, CA, USA, 2001; ISBN 978-0-520-22393-6.
3. Bocquet-Appel, J.-P.; Tuffreau, A. Technological Responses of Neanderthals to Macroclimatic Variations (240,000–40,000 BP). *Hum. Biol.* **2009**, *81*, 287–307. [[CrossRef](#)] [[PubMed](#)]



4. Banks, W.E.; d'Errico, F.; Zilhão, J. Human-Climate Interaction during the Early Upper Paleolithic: Testing the Hypothesis of an Adaptive Shift between the Proto-Aurignacian and the Early Aurignacian. *J. Hum. Evol.* **2013**, *64*, 39–55. [[CrossRef](#)] [[PubMed](#)]
5. Kelly, R.L. *The Lifeways of Hunter-Gatherers: The Foraging Spectrum*, 2nd ed.; Cambridge University Press: New York, NY, USA, 2013.
6. Vignoles, A. Trajectoires Technologiques et Dynamiques de Niches Éco-Culturelles Du Gravettien Moyen Au Gravettien Récent En France. Unpublished. Ph.D. Dissertation, University of Bordeaux, Bordeaux, France, 2021.
7. Sanchez Goñi, M.-F.; Turon, J.-L.; Eynaud, F.; Gendreau, S. European Climatic Response to Millennial-Scale Changes in the Atmosphere–Ocean System during the Last Glacial Period. *Quat. Res.* **2000**, *54*, 394–403. [[CrossRef](#)]
8. Hemming, S.R. Heinrich Events: Massive Late Pleistocene Detritus Layers of the North Atlantic and Their Global Climate Imprint. *Rev. Geophys.* **2004**, *42*. [[CrossRef](#)]
9. Lynch-Stieglitz, J.; Schmidt, M.W.; Gene Henry, L.; Curry, W.B.; Skinner, L.C.; Mulitza, S.; Zhang, R.; Chang, P. Muted Change in Atlantic Overturning Circulation over Some Glacial-Aged Heinrich Events. *Nat. Geosci.* **2014**, *7*, 144–150. [[CrossRef](#)]
10. Parker, A.O.; Schmidt, M.W.; Chang, P. Tropical North Atlantic Subsurface Warming Events as a Fingerprint for AMOC Variability during Marine Isotope Stage 3. *Paleoceanography* **2015**, *30*, 1425–1436. [[CrossRef](#)]
11. Turney, C.S.M.; Palmer, J.; Bronk Ramsey, C.; Adolphi, F.; Muscheler, R.; Hughen, K.A.; Staff, R.A.; Jones, R.T.; Thomas, Z.A.; Fogwill, C.J.; et al. High-Precision Dating and Correlation of Ice, Marine and Terrestrial Sequences Spanning Heinrich Event 3: Testing Mechanisms of Interhemispheric Change Using New Zealand Ancient Kauri (*Agathis Australis*). *Quat. Sci. Rev.* **2016**, *137*, 126–134. [[CrossRef](#)]
12. Touzé, O. De La Signification Du Noaillien et Du Rayssien. In *Pensando el Gravetiense: Nuevos datos para la región cantábrica en su contexto peninsular y pirenaico*; de las Heras, C., Lasheras, J.A., Arrizabalaga, Á., de la Rasilla, M., Eds.; Monografías del Museo Nacional y Centro de Investigación de Altamira; Museo Nacional y Centro de Investigación de Altamira: Madrid, Spain, 2013; pp. 383–400.
13. Bricker, H.M. *Le Paléolithique Supérieur de l'abri Pataud (Dordogne): Les Fouilles de H. L. Movius Jr.*; Documents d'archéologie française; Maison des sciences de l'homme: Paris, France, 1995.
14. David, N.C. Excavation of the Abri Pataud, Les Eyzies (Dordogne): The Noaillian (Level 4) Assemblage and the Noaillian Culture in Western Europe. In *Bulletin (American School of Prehistoric Research)*; Harvard University Press: Cambridge, MA, USA, 1985.
15. Bosselin, B.; Djindjian, F. La Chronologie Du Gravettien Français. *Préhistoire Eur.* **1994**, *6*, 77–115.
16. Klaric, L. L'unité technique des industries à burins du Raysse dans leur contexte diachronique. Réflexions sur la variabilité culturelle au Gravettien à partir des exemples de la Picardie, d'Arcy-sur-Cure, de Brassempouy et du Cirque de la Patrie. Unpublished. Ph.D. Dissertation, Université Panthéon-Sorbonne—Paris I, Paris, France, 2003.
17. Klaric, L.; Goutas, N.; Lacarrière, J.; Banks, W.E. Rayssien? Vous avez dit Rayssien? Approche multi-proxies d'une culture préhistorique. In *Les sociétés gravettiennes du Nord-Ouest européen: Nouveaux sites, nouvelles données, nouvelles lectures*; Etudes et recherches archéologiques de l'Université de Liège; Presses Universitaires de Liège: Liège, Belgium, 2021; pp. 323–366.
18. Vignoles, A.; Caillo, A.; Banks, W.E.; Klaric, L. Une Base de Données Bibliographique Critique Pour Estimer La Répartition Géographique Des Traditions Techniques Lithiques Du Gravettien Moyen et Récent En France. *Bull. Société Préhistorique Française*, **2024**; *in press*.
19. Primault, J.; Gabelleau, J.; Brou, L.; Griggo, C.; Henry-Gambier, D.; Houmard, C.; Laroulandie, V.; le Brun-Ricalens, F.; Liolios, D.; Mistrot, V.; et al. Le Magdalénien inférieur à microlamelles à dos de la grotte du Taillis des Coteaux à Antigny (Vienne, France). *Bull. Société Préhistorique Française* **2007**, *104*, 5–30. [[CrossRef](#)]
20. Waelbroeck, C.; Labeyrie, L.; Michel, E.; Duplessy, J.C.; McManus, J.F.; Lambeck, K.; Balbon, E.; Labracherie, M. Sea-Level and Deep Water Temperature Changes Derived from Benthic Foraminifera Isotopic Records. *Quat. Sci. Rev.* **2002**, *21*, 295–305. [[CrossRef](#)]
21. Pottier, C.; De Araujo Igreja, M.; Bracco, J.-P.; Le Brun-Ricalens, F. Productions Lamellaires et Burins Du Raysse Du Gravettien Moyen de l'Abri Pataud (Dordogne, France). In *Burins Préhistoriques: Formes, Fonctionnements, Fonctions*; Archéologiques 2: Luxembourg, 2006; pp. 121–140.
22. Klaric, L. « La Réussite d'une Production Repose Sur l'attention Prêtée Aux Détails »: L'exemple Des Débitages Lamellaires Par Méthode Du Raysse (Gravettien Moyen, France). *J. Lithic Stud.* **2017**, *4*, 387–421. [[CrossRef](#)]
23. Klaric, L. Anciennes et Nouvelles Hypothèses d'interprétation Du Gravettien Moyen En France: La Question de La Place Des Industries à Burins Du Raysse Au Sein de La Mosaïque Gravettienne. *PALEO. Rev. D'archéologie Préhistorique* **2008**, *20*, 257–276. [[CrossRef](#)]
24. Vignoles, A.; Klaric, L.; Banks, W.E.; Baumann, M. Le Gravettien Du Fourneau Du Diable (Bourdeilles, Dordogne): Révision Chronoculturelle Des Ensembles Lithiques de La "Terrasse Inférieure." *Bull. Société Préhistorique Française* **2019**, *116*, 455–478. [[CrossRef](#)]
25. Vignoles, A. Le mythe du site de référence: Décalage entre publication et réalité. In *Imagination et construction mentale. La fabrique du discours scientifique*; Orellana-González, E., Spinelli Sanchez, O., Balbin-Estanguet, T., Sergues, V., Taffin, N., Eds.; Ausonius editions: Pessac, France, 2022; pp. 17–32, ISBN 9782356135032. Available online: <https://una-editions.fr/le-mythe-du-site-de-reference/> (accessed on 26 July 2023).
26. Guillermin, P. Les «Périgordiens» En Quercy: L'exemple Du Gisement Des Fieux. *PALEO. Rev. D'archéologie Préhistorique* **2008**, *20*, 357–372. [[CrossRef](#)]

27. Rigaud, J.-P.; Simek, J.; Delpech, F.; Texier, J.-P. L'Aurignacien et le Gravettien du nord de l'Aquitaine: La contribution du Flageolet I (Bézenac, Dordogne, France). *PALEO. Rev. D'archéologie Préhistorique* **2016**, 265–295. [[CrossRef](#)]
28. Touzé, O. Nouveau Regard Sur Le Gravettien de La « Clairière Est » Du Cirque de La Patrie. Etude Typo-Technologique d'une Industrie à Pièces Pédonculées Du Nord-Ouest Européen. Unpublished. Master's Thesis, University of Paris 1—Panthéon-Sorbonne, Paris, France, 2013.
29. Klaric, L. Regional Groups in the European Middle Gravettian: A Reconsideration of the Rayssian Technology. *Antiquity* **2007**, *81*, 176–190. [[CrossRef](#)]
30. David, N.; Bricker, H.M. Perigordian and Noaillian in the Greater Perigord. In *The Pleistocene Old World: Regional Perspectives*; Soffer, O., Ed.; Plenum Press: New York, NY, USA, 1987; pp. 237–250.
31. Djindjian, F.; Bosselin, B. Périgordien et Gravettien: L'épilogue d'une Contradiction ? *Préhistoire Eur.* **1994**, *6*, 117–131.
32. Pottier, C. Le Gravettien Moyen de l'abri Pataud (Dordogne, France): Le Niveau 4 et l'éboulis 3/4. Etude Typologique et Technologique de l'industrie Lithique. Unpublished. Ph.D. Dissertation, Muséum National d'Histoire Naturelle, Paris, France, 2005.
33. Rigaud, J.-P. Le Paléolithique En Périgord: Les Données Du Sud-Ouest Sarladais et Leurs Implications. Ph.D. Dissertation, University of Bordeaux, Talence, France, 1982.
34. Rigaud, J.-P. The Gravettian Peopling of Southwestern France: Taxonomic Problems. In *Upper Pleistocene Prehistory of Western Eurasia*; Dibble, H.L., Montet-White, A., Eds.; University Museum Monographs; The University Museum, University of Pennsylvania: Philadelphia, PA, USA, 1988; pp. 387–396.
35. Rigaud, J.-P. Les industries lithiques du Gravettien du nord de l'Aquitaine dans leur cadre chronologique. *PALEO. Rev. D'archéologie Préhistorique* **2008**, *20*, 381–398. [[CrossRef](#)]
36. Vignoles, A.; Banks, W.E.; Klaric, L.; Kageyama, M.; Cobos, M.E.; Romero-Alvarez, D. Investigating Relationships between Technological Variability and Ecology in the Middle Gravettian (ca. 32–28 Ky Cal. BP) in France. *Quat. Sci. Rev.* **2021**, *253*, 106766. [[CrossRef](#)]
37. Douka, K.; Chiotti, L.; Nespoulet, R.; Higham, T. A Refined Chronology for the Gravettian Sequence of Abri Pataud. *J. Hum. Evol.* **2020**, *141*, 102730. [[CrossRef](#)] [[PubMed](#)]
38. Ducasse, S.; Pétilon, J.-M.; Aubry, T.; Chauvière, F.-X.; Castel, J.-C.; Detrain, L.; Langlais, M.; Morala, A.; Banks, W.E.; Lenoble, A. The Abri Casserole (Dordogne, France): Reassessing the 14C Chronology of a Key Upper Paleolithic Sequence in Southwestern France. *Radiocarbon* **2020**, *62*, 1237–1260. [[CrossRef](#)]
39. Rigaud, J.P. Aquitaine. *Gall. Préhistoire* **1986**, *29*, 233–258.
40. Morala, A. La Spécialisation Des Activités: Concept de l'archéologue et Réalité Archéologique; Les Données Du Site Gravettien Moyen Du Callan (Lot-et-Garonne). In *À la recherche des identités gravettiennes: Actualités, questionnements et perspectives*; Goutas, N., Klaric, L., Pesesse, D., Guillermin, P., Eds.; Memoire de la SPF; Société Préhistorique Française: Paris, France, 2011; pp. 343–358.
41. Peyrony, E. Le Gisement de La Forêt, Commune de Tursac (Dordogne). In Proceedings of the Congrès Préhistorique de France XI, Périgueux, France, 16–22 September 1934; pp. 424–430.
42. Delporte, H. L'abri du Facteur à Tursac (Dordogne). I. Etude générale. *Gall. Préhistoire* **1968**, *11*, 1–112. [[CrossRef](#)]
43. Simonet, A. Les Gravettiens Des Pyrénées: Des Armes Aux Sociétés. Unpublished. Ph.D. Dissertation, University of Toulouse-Jean Jaurès, Toulouse, France, 2009.
44. Lucas, G. Les Industries Lithiques Du Flageolet I (Dordogne): Approche Économique, Technologique, Fonctionnelle et Analyse Spatiale. Unpublished. Ph.D. Dissertation, University of Bordeaux 1, Talence, France, 2000.
45. Gottardi, G. La Question Des Faciès Au Gravettien: Fonctions, Traditions Ou Chronologie ? Unpublished. Master's Thesis, University of Bordeaux 1, Talence, France, 2011.
46. Célérier, G. Le gisement périgordien supérieur des "Jambes", commune de Périgueux (Dordogne). *Bull. Société Préhistorique Française* **1967**, *64*, 53–68. [[CrossRef](#)]
47. Klaric, L.; Liard, M.; Bertran, P.; Dumarçay, G.; de Araujo-Igreja, M.; Aubry, T.; Walter, B.; Regert, M. La Picardie (Preuilysur-Claise, Indre-et-Loire): Neuf Ans de Fouille Sur Un Gisement Rayssien Finalement Pas Si Mal Conservé ! In *À la recherche des identités gravettiennes: Actualités, questionnements et perspectives*; Goutas, N., Klaric, L., Pesesse, D., Guillermin, P., Eds.; Memoire de la SPF; Société Préhistorique Française: Paris, France, 2011; pp. 291–310.
48. Klaric, L.; Bertran, P.; Dumarçay, G.; Liard, M. A Long and Winding Road: Towards a Palethnographic Interpretation of the Middle-Gravettian Site of La Picardie (Indre-et-Loire, France). *Quat. Int.* **2018**, *498*, 51–68. [[CrossRef](#)]
49. Klaric, L.; Aubry, T.; Walter, B. Un Nouveau Type d'armature En Contexte Gravettien et Son Mode de Production Sur Les Burins Du Raysse (La Picardie, Commune de Preuilysur-Claise, Indre-et-Loire). *Bull. Société Préhistorique Française* **2002**, *99*, 751–764. [[CrossRef](#)]
50. Brock, F.; Higham, T.; Ditchfield, P.; Ramsey, C.B. Current Pretreatment Methods for AMS Radiocarbon Dating at the Oxford Radiocarbon Accelerator Unit (Orau). *Radiocarbon* **2010**, *52*, 103–112. [[CrossRef](#)]
51. Dee, M.; Bronk Ramsey, C. Refinement of Graphite Target Production at ORAU. *Nucl. Instrum. Methods Phys. Res. Sect. B Beam Interact. Mater. At.* **2000**, *172*, 449–453. [[CrossRef](#)]
52. Bronk Ramsey, C.; Higham, T.; Leach, P. Towards High-Precision AMS: Progress and Limitations. *Radiocarbon* **2004**, *46*, 17–24. [[CrossRef](#)]
53. Naylor, J.C.; Smith, A.F.M. An Archaeological Inference Problem. *J. Am. Stat. Assoc.* **1988**, *83*, 588–595. [[CrossRef](#)]

54. Buck, C.E.; Litton, C.D.; Smith, A.F.M. Calibration of Radiocarbon Results Pertaining to Related Archaeological Events. *J. Archaeol. Sci.* **1992**, *19*, 497–512. [[CrossRef](#)]
55. Christen, J.A. Summarizing a Set of Radiocarbon Determinations: A Robust Approach. *J. R. Stat. Society. Ser. C (Appl. Stat.)* **1994**, *43*, 489–503. [[CrossRef](#)]
56. Litton, C.D.; Buck, C.E. The Bayesian Approach to the Interpretation of Archaeological Data. *Archaeometry* **1995**, *37*, 1–24. [[CrossRef](#)]
57. Bronk Ramsey, C. Bayesian Analysis of Radiocarbon Dates. *Radiocarbon* **2009**, *51*, 337–360. [[CrossRef](#)]
58. Lanos, P.; Philippe, A. Event Date Model: A Robust Bayesian Tool for Chronology Building. *Commun. Stat. Appl. Methods* **2018**, *25*, 131–157. [[CrossRef](#)]
59. Lanos, P.; Philippe, A. Hierarchical Bayesian modeling for combining dates in archeological context. *J. Société Française Stat.* **2017**, *158*, 72–88.
60. Higham, T.; Douka, K.; Wood, R.; Ramsey, C.B.; Brock, F.; Basell, L.; Camps, M.; Arrizabalaga, A.; Baena, J.; Barroso-Ruiz, C.; et al. The Timing and Spatiotemporal Patterning of Neanderthal Disappearance. *Nature* **2014**, *512*, 306–309. [[CrossRef](#)] [[PubMed](#)]
61. Cascalheira, J.; Bicho, N. On the Chronological Structure of the Solutrean in Southern Iberia. *PLoS ONE* **2015**, *10*, e0137308. [[CrossRef](#)]
62. Lanos, P.; Dufresne, P. *Chronomodel Version 2.0: Software for Chronological Modelling of Archaeological Data Using Bayesian Statistics*; Centre National de la Recherche Scientifique: Paris, France, 2019.
63. Buck, C.; Christen, J.A.; James, G.N. BCal: An on-Line Bayesian Radiocarbon Calibration Tool. *Internet Archaeol.* **1999**, *7*. [[CrossRef](#)]
64. Bronk Ramsey, C. Development of the Radiocarbon Calibration Program. *Radiocarbon* **2001**, *43*, 355–363. [[CrossRef](#)]
65. Reimer, P.J.; Austin, W.E.N.; Bard, E.; Bayliss, A.; Blackwell, P.G.; Ramsey, C.B.; Butzin, M.; Cheng, H.; Edwards, R.L.; Friedrich, M.; et al. The IntCal20 Northern Hemisphere Radiocarbon Age Calibration Curve (0–55 Cal kBP). *Radiocarbon* **2020**, *62*, 725–757. [[CrossRef](#)]
66. Lavelle, H.; Rigaud, J.-P. The Perigordian V Industries in Périgord: Typological Variation, Stratigraphy, Relative Chronology. *World Archaeol.* **1973**, *4*, 330–338. [[CrossRef](#)]
67. Higham, T.; Jacobi, R.; Basell, L.; Ramsey, C.B.; Chiotti, L.; Nespoulet, R. Precision Dating of the Palaeolithic: A New Radiocarbon Chronology for the Abri Pataud (France), a Key Aurignacian Sequence. *J. Hum. Evol.* **2011**, *61*, 549–563. [[CrossRef](#)]
68. Rasmussen, S.O.; Bigler, M.; Blockley, S.P.; Blunier, T.; Bucharadt, S.L.; Clausen, H.B.; Cvijanovic, I.; Dahl-Jensen, D.; Johnsen, S.J.; Fischer, H.; et al. A Stratigraphic Framework for Abrupt Climatic Changes during the Last Glacial Period Based on Three Synchronized Greenland Ice-Core Records: Refining and Extending the INTIMATE Event Stratigraphy. *Quat. Sci. Rev.* **2014**, *106*, 14–28. [[CrossRef](#)]
69. Naughton, F.; Sánchez Goñi, M.F.; Kageyama, M.; Bard, E.; Duprat, J.; Cortijo, E.; Desprat, S.; Malaizé, B.; Joly, C.; Rostek, F.; et al. Wet to Dry Climatic Trend in North-Western Iberia within Heinrich Events. *Earth Planet. Sci. Lett.* **2009**, *284*, 329–342. [[CrossRef](#)]
70. Sánchez Goñi, M.F.; Landais, A.; Fletcher, W.J.; Naughton, F.; Desprat, S.; Duprat, J. Contrasting Impacts of Dansgaard–Oeschger Events over a Western European Latitudinal Transect Modulated by Orbital Parameters. *Quat. Sci. Rev.* **2008**, *27*, 1136–1151. [[CrossRef](#)]
71. Fletcher, W.J.; Sánchez Goñi, M.F.; Allen, J.R.M.; Cheddadi, R.; Combourieu-Nebout, N.; Huntley, B.; Lawson, I.; Londeix, L.; Magri, D.; Margari, V.; et al. Millennial-Scale Variability during the Last Glacial in Vegetation Records from Europe. *Quat. Sci. Rev.* **2010**, *29*, 2839–2864. [[CrossRef](#)]
72. Badino, F.; Pini, R.; Bertuletti, P.; Ravazzi, C.; Delmonte, B.; Monegato, G.; Reimer, P.; Vallé, F.; Arrighi, S.; Bortolini, E.; et al. The Fast-Acting “Pulse” of Heinrich Stadial 3 in a Mid-Latitude Boreal Ecosystem. *Sci. Rep.* **2020**, *10*, 18031. [[CrossRef](#)]
73. Allen, J.R.M.; Forrest, M.; Hickler, T.; Singarayer, J.S.; Valdes, P.J.; Huntley, B. Global Vegetation Patterns of the Past 140,000 Years. *J. Biogeogr.* **2020**, *47*, 2073–2090. [[CrossRef](#)]
74. Antoine, P.; Goval, E.; Jamet, G.; Coutard, S.; Moine, O.; Hérisson, D.; Auguste, P.; Guérin, G.; Lacroix, F.; Schmidt, E.; et al. Les séquences loessiques pléistocène supérieur d’Havrincourt (Pas-de-Calais, France): Stratigraphie, paléoenvironnements, géochronologie et occupations paléolithiques. *Quat. Rev. l’Association française pour l’étude Quat.* **2014**, *25*, 321–368. [[CrossRef](#)]
75. Bertran, P.; Andrieux, E.; Antoine, P.; Coutard, S.; Deschodt, L.; Gardère, P.; Hernandez, M.; Legentil, C.; Lenoble, A.; Liard, M.; et al. Distribution and Chronology of Pleistocene Permafrost Features in France: Database and First Results. *Boreas* **2014**, *43*, 699–711. [[CrossRef](#)]
76. Andrieux, E.; Bateman, M.D.; Bertran, P. The Chronology of Late Pleistocene Thermal Contraction Cracking Derived from Sand Wedge OSL Dating in Central and Southern France. *Glob. Planet. Chang.* **2018**, *162*, 84–100. [[CrossRef](#)]
77. Bosq, M.; Kreutzer, S.; Bertran, P.; Lanos, P.; Dufresne, P.; Schmidt, C. Last Glacial Loess in Europe: Luminescence Database and Chronology of Deposition. *Earth Syst. Sci. Data* **2023**, *15*, 4689–4711. [[CrossRef](#)]
78. Bleed, P. The Optimal Design of Hunting Weapons: Maintainability or Reliability. *Am. Antiq.* **1986**, *51*, 737–747. [[CrossRef](#)]
79. Shott, M.J. An Exegesis of the Curation Concept. *J. Anthropol. Res.* **1996**, *52*, 259–280. [[CrossRef](#)]
80. Klaric, L.; Guillermin, P.; Aubry, T. Des armatures variées et des modes de productions variables. Réflexions à partir de quelques exemples issus du Gravettien d’Europe occidentale (France, Portugal, Allemagne). *Gall. Préhistoire* **2009**, *51*, 113–154. [[CrossRef](#)]
81. Lacarrière, J. Les Ressources Cynégétiques Au Gravettien En France: Acquisition et Modalités d’exploitation Des Animaux Durant La Phase d’instabilité Climatique Précédant Le Dernier Maximum Glaciaire. Unpublished. Ph.D. Dissertation, University of Toulouse-Jean Jaurès, Toulouse, France, 2015.

82. Cho, T. Étude archéozoologique de la faune du Périgordien supérieur (couches 2, 3, 4) de l'abri Pataud (Les Eyzies-de-Tayac, Dordogne): Paléocéologie, taphonomie, paleoéconomie. Unpublished. Ph.D. Dissertation, Muséum National d'Histoire Naturelle, Paris, France, 1998.
83. Paris, C. La période du Gravettien dans la zone loessique du Nord de la France: Traditions culturelles et dynamiques de peuplement. Unpublished. Ph.D. Dissertation, University of Paris 1—Panthéon-Sorbonne, Paris, France, 2020.
84. Antoine, P.; Coutard, S.; Guerin, G.; Deschodt, L.; Goval, E.; Loch, J.-L.; Paris, C. Upper Pleistocene Loess-Palaeosol Records from Northern France in the European Context: Environmental Background and Dating of the Middle Palaeolithic. *Quat. Int.* **2016**, *411*, 4–24. [[CrossRef](#)]
85. Kelly, R.L. Colonization of New Land by Hunter-Gatherers: Expectations and Implications Based on Ethnographic Data. In *Colonization of Unfamiliar Landscapes: The Archaeology of Adaptation*; Rockman, M., Steele, J., Eds.; Routledge: New York, NY, USA, 2003; pp. 44–58.
86. Bodu, P.; Baillet, M.; Ballinger, M.; Dumarçay, G.; Goutas, N.; Julien, M.-A.; Lacarrière, J.; Legrand-Pineau, A.; Lejay, M.; Leroyer, M.; et al. Le Gisement Paléolithique Multistratifié « les Bossats » à Ormesson (Seine-et-Marne, France): Palethnographie Ou Pâle Ethnographie ? Une Synthèse Des Huit Premières Années de Fouille (2009-2016). In *Préhistoire de l'Europe du Nord-Ouest: Mobilités, Climats et Identités Culturelles. XXVIIIe Congrès Préhistorique de France*; Montoya, C., Fagnart, J.-P., Loch, J.-L., Eds.; Congrès Préhistorique de France: Amiens, France, 2019; Volume 2, pp. 231–262.
87. Foucher, P.; San Juan, C.; Valladas, H.; Clottes, J.; Begouën, R.; Giraud, J.-P. De Nouvelles Dates 14C Pour Le Gravettien Des Pyrénées Centrales. *Bull. Société Préhistorique Ariège-Pyrénées* **2001**, *56*, 35–44.
88. Foucher, P.; San Juan, C.; Martin, H. Le Site Gravettien de La Carane-3 Foix, Ariège. *Bull. Société Préhistorique Ariège-Pyrénées* **2000**, *54*, 15–42.
89. Foucher, P.; San Juan-Foucher, C.; Oberlin, C. Les Niveaux d'occupation Gravettiens de Gargas (Hautes-Pyrénées): Nouvelles Données Chronostratigraphiques. In *À la Recherche des Identités Gravettiennes: Actualités, Questionnements, Perspectives*; Goutas, N., Klaric, L., Pesesse, D., Guillermin, P., Eds.; Mémoire; Société Préhistorique française: Paris, France, 2011; pp. 373–385.
90. Mellars, P.A.; Bricker, H.M.; Gowlett, J.A.J.; Hedges, R.E.M. Radiocarbon Accelerator Dating of French Upper Palaeolithic Sites. *Curr. Anthropol.* **1987**, *28*, 128–133. [[CrossRef](#)]
91. Higham, T.; Jacobi, R.; Julien, M.; David, F.; Basell, L.; Wood, R.; Davies, W.; Ramsey, C.B. Chronology of the Grotte Du Renne (France) and Implications for the Context of Ornaments and Human Remains within the Châtelperronian. *Proc. Natl. Acad. Sci.* **2010**, *107*, 20234–20239. [[CrossRef](#)] [[PubMed](#)]
92. Gowlett, J.A.J.; Hedges, R.E.M.; Law, I.A.; Perry, C. Radiocarbon Dates from the Oxford Ams System: Archaeometry Datalog 5. *Archaeometry* **1987**, *29*, 125–155. [[CrossRef](#)]
93. Primault, J.; Berthet, A.-L.; Brou, L.; Delfour, G.; Gabilleau, J.; Griggo, C.; Guérin, S.; Henry-Gambier, D.; Houmard, C.; Jeannet, M.; et al. La grotte du Taillis des Coteaux à Antigny (Vienne). In *Préhistoire entre Vienne et Charente: Hommes et Sociétés du Paléolithique*; Buisson-Catil, J., Primault, J., Eds.; Mémoire; Association des Publications Chauvinoises: Chauvigny, France, 2010; pp. 271–293.
94. Delvigne, V. Géorressources et Expressions Technoculturelles Dans Le Sud Du Massif Central Au Paléolithique Supérieur: Des Déterminismes et Des Choix. Unpublished. Ph.D. Dissertation, University of Bordeaux, Talence, France, 2016.
95. Verpoorte, A.; Cosgrove, R.; Wood, R.; Petchey, F.; Lenoble, A.; Chadelle, J.-P.; Smith, C.; Kamermans, H.; Roebroeks, W. Improving the Chronological Framework for Laugerie-Haute Ouest (Dordogne, France). *J. Archaeol. Sci. Rep.* **2019**, *23*, 574–582. [[CrossRef](#)]
96. Allard, M. Habitats Gravettiens Sous l'abri Des Peyrugues (Orniac, Lot) Entre 25000 BP et 22000 BP. In *À la recherche des identités gravettiennes: Actualités, questionnements, perspectives*; Goutas, N., Klaric, L., Pesesse, D., Guillermin, P., Eds.; Mémoire de la SPF; Société préhistorique française: Paris, France, 2011; pp. 359–372.
97. Paris, C.; Fagnart, J.-P.; Coudret, P. Du Gravettien final dans le Nord de la France ? Nouvelles données à Amiens-Renancourt (Somme, France). *Bull. Société Préhistorique Française* **2013**, *110*, 123–126. [[CrossRef](#)]
98. Fagnart, J.-P.; Coudret, P.; ANTOINE, P.; Vallin, L.; Sellier, N.; Masson, B. Le Paléolithique Supérieur Ancien Dans Le Nord de La France. In *Le Paléolithique supérieur ancien de l'Europe du Nord-Ouest. Réflexions et synthèses à partir d'un projet collectif de recherche sur le Centre et le Sud du Bassin parisien*; Bodu, P., Chehmana, L., Klaric, L., Mevel, L., Soriano, S., Teyssandier, N., Eds.; Mémoire de la SPF; Société préhistorique française: Paris, France, 2013; pp. 197–214.
99. Paris, C.; Deneuve, E.; Fagnart, J.-P.; Coudret, P.; Antoine, P.; Peschaux, C.; Lacarrière, J.; Coutard, S.; Moine, O.; Guérin, G. Premières observations sur le gisement gravettien à statuettes féminines d'Amiens-Renancourt 1 (Somme). *Bull. Société Préhistorique Française* **2017**, *114*, 423–444. [[CrossRef](#)]
100. Surmely, F.; Hays, M. Nouvelles Données Sur Les Industries Lithiques Des Niveaux Protomagdaléniens Du Site Du Blot (Cerzat, Haute-Loire). In *À la Recherche des Identités Gravettiennes: Actualités, Questionnements, Perspectives*; Goutas, N., Klaric, L., Pesesse, D., Guillermin, P., Eds.; Mémoire de la SPF; Société Préhistorique française: Paris, France, 2011; pp. 111–127.
101. Lenoble, A.; Cosgrove, R. Les Eyzies-de-Tayac-Sireuil – Laugerie-Haute Ouest. *ADLFI. Archéologie de la France - Informations* **2012**, 41–42. [[CrossRef](#)]
102. Nespoulet, R.; Chiotti, L.; Henry-Gambier, D. *Le Gravettien Final de l'abri Pataud (Dordogne, France)*; BAR International Series; Archaeopress: Oxford, UK, 2013.
103. Aubry, T.; Walter, B.; Peyrouse, J.-B. Paléolithique Moyen et Supérieur de La Vallée de La Claise: Bilan de Vingt Ans d'étude et Nouvelles Perspectives. *Bull. Amis Musée Préhistoire Grand-Press.* **2014**, *65*, 9–29.

104. Allard, M.; Chalard, P.; Jeannet, M.; Juillard, F.; Le Gall, O.; Pommies, M.P.; Alix, P.; Goupil, S.; Jarry, M. *Les Peyrugues (Orniac, Lot). Rapport de Synthèse, Fouille Programmée 1994–1996*; SRA Midi-Pyrénées: Toulouse, France, 1996.
105. Roque, C.; Guibert, P.; Vartanian, E.; Bechtel, F.; Oberlin, C.; Evin, J.; Mercier, N.; Valladas, H.; Texier, J.-P.; Rigaud, J.-P.; et al. Une Expérience de Croisement de Datations TL/14C Pour La Séquence Solutrénienne de Laugerie-Haute, Dordogne. In *XXI Rencontres Internationales d'Archeologie et d'Histoire d'Antibes, Antibes, France, 19–21 October 2000*; Barrandon, J.-N., Guibert, P., Michel, V., Eds.; Editions APDCA (Association pour la Promotion et la Diffusion des Connaissances Archéologiques: Antibes, France, 2001; pp. 217–232.
106. Bodu, P.; Dumarçay, G.; Naton, H.-G. Un nouveau gisement solutréen en Île-de-France, le site des Bossats à Ormesson (Seine-et-Marne). *Bull. Société Préhistorique Française* **2014**, *111*, 225–254. [[CrossRef](#)]
107. Ducasse, S.; Pétillon, J.-M.; Renard, C. Le cadre radiométrique de la séquence solutréo-badegoulienne du Cuzoul de Vers (Lot, France): Lecture critique et compléments. *PALEO. Rev. D'archéologie Préhistorique* **2014**, *25*, 37–58. [[CrossRef](#)]
108. Ducasse, S.; Castel, J.-C.; Chauvière, F.-X.; Langlais, M.; Camus, H.; Morala, A.; Turq, A. Le Quercy au cœur du dernier maximum glaciaire. La couche 4 du Petit Cloup Barrat et la question de la transition badegoulo-magdalénienne. *PALEO. Rev. D'archéologie Préhistorique* **2011**, *22*, 101–154.
109. Hinguant, S.; Colleter, R. *Le Solutrén de La Grotte Rochefort (Saint-Pierre-Sur-Erve, Mayenne)*; SRA Pays de la Loire: Rennes, France, 2010; p. 213.
110. Montet-White, A.; Evin, J.; Stafford, T. Les Datations Radiocarbone Des Amas Osseux de Solutré. In *Solutré: 1968–1998*; Combier, J., Montet-White, A., Eds.; Mémoire de la SPF; Société préhistorique française: Paris, France, 2002; pp. 181–189.
111. BANADORA Banque Nationale de Données Radiocarbone: Pour l'Europe et Le Proche Orient. 2018. BANADORA: Banque Nationale de Donnée Radiocarbone. Available online: <https://www.arar.mom.fr/banadora/> (accessed on 1 October 2018).
112. Lafarge, A. Entre Plaine et Montagne: Techniques et Cultures Du Badegoulien Du Massif Central, de l'Allier Au Velay. Unpublished. Ph.D. Dissertation, University of Montpellier III, Montpellier, France, 2014.
113. Pétillon, J.-M.; Ducasse, S. From Flakes to Grooves: A Technical Shift in Antlerworking during the Last Glacial Maximum in Southwest France. *J. Hum. Evol.* **2012**, *62*, 435–465. [[CrossRef](#)] [[PubMed](#)]
114. Ducasse, S.; Pétillon, J.-M.; Chauvière, F.-X.; Renard, C.; Lacrampe-Cuyaubère, F.; Muth, X. Archaeological Recontextualization and First Direct 14C Dating of a “Pseudo-Excise” Decorated Antler Point from France (Pégourié Cave, Lot). Implications on the Cultural Geography of Southwestern Europe during the Last Glacial Maximum. *J. Archaeol. Sci. Rep.* **2019**, *23*, 592–616. [[CrossRef](#)]
115. Raynal, J.-P.; Lafarge, A.; Rémy, D.; Delvigne, V.; Guadelli, J.-L.; Costamagno, S.; Le Gall, O.; Daujeard, C.; Vivent, D.; Fernandes, P.; et al. Datations SMA et Nouveaux Regards Sur l'archéo-Séquence Du Rond-Du-Barry (Polignac, Haute-Loire). *Comptes Rendus. Palevol.* **2014**, *13*, 623–636. [[CrossRef](#)]
116. Debout, G.; Olive, M.; Bignon, O.; Bodu, P.; Chehmana, L.; Valentin, B. The Magdalenian in the Paris Basin: New Results. *Quat. Int.* **2012**, *272–273*, 176–190. [[CrossRef](#)]
117. Bazile, F. Datations du site de Fontgrasse (Vers-Pont-Du-Gard, Gard.) Implications sur la phase ancienne du Magdalénien en France Méditerranéenne. *Bull. Société Préhistorique Française* **2006**, *103*, 597–602. [[CrossRef](#)]
118. Tisnerat-Laborde, N.; Valladas, H.; Ladier, E. Nouvelles Datations Carbone 14 En SMA Pour Le Magdalénien Supérieur de La Vallée de l'Aveyron. *Bull. Société Préhistoire Ariège-Pyrénées* **1997**, *2*, 129–136.
119. Langlais, M.; Ladier, E.; Chalard, P.; Jarry, M.; Lacrampe-Cuyaubère, F. Aux origines du Magdalénien « classique »: Les industries de la séquence inférieure de l'Abri Gandil (Bruniquel, Tarn-et-Garonne). *PALEO. Rev. D'archéologie Préhistorique* **2007**, *19*, 341–366. [[CrossRef](#)]
120. Barshay-Szmidt, C.; Costamagno, S.; Henry-Gambier, D.; Laroulandie, V.; Pétillon, J.-M.; Boudadi-Maligne, M.; Kuntz, D.; Langlais, M.; Mallye, J.-B. New Extensive Focused AMS 14C Dating of the Middle and Upper Magdalenian of the Western Aquitaine/Pyrenean Region of France (ca. 19–14 Ka Cal BP): Proposing a New Model for Its Chronological Phases and for the Timing of Occupation. *Quat. Int.* **2016**, *414*, 62–91. [[CrossRef](#)]
121. Lenoir, M.; Marmier, F.; Trécolle, G. Le Gisement Magdalénien de Saint-Germain-La-Rivière (Gironde): Données Anciennes et Acquis Récents. *Rev. Archéologique Bordx.* **1994**, *85*, 39–72.

**Disclaimer/Publisher's Note:** The statements, opinions and data contained in all publications are solely those of the individual author(s) and contributor(s) and not of MDPI and/or the editor(s). MDPI and/or the editor(s) disclaim responsibility for any injury to people or property resulting from any ideas, methods, instructions or products referred to in the content.